

## ESI to: Oxidations of chromene-annulated chlorin

Nisansala Hewage, Matthias Zeller, and Christian Brückner\*

*Department of Chemistry, University of Connecticut, Storrs, CT 06269-3060 USA. Department of Chemistry, Youngstown State University, One University Plaza, Youngstown, OH 44555-3663, United States*

### Table of Contents

CrO <sub>3</sub> Oxidation of 5,10,15,20-Tetrakis(pentafluorophenyl)-2,3- <i>cis</i> -dihydroxychlorin ( <b>2<sup>F</sup></b> ).....	2
5,10,15,20-Tetrakis(pentafluorophenylporpholactone <b>4<sup>F</sup></b> – Known compound, included for reference .....	2
<i>meso</i> -Tetrakis(pentafluorophenyl)-2,3-dioxoporphyrin ( <b>3<sup>F</sup></b> ).....	5
10,15,20-Tris(pentafluorophenyl)-5-(tetrafluorochromene-annulated)-3-hydroxy-2-oxo-chlorin ( <b>15<sup>OH</sup></b> ) .....	10
5-(2'-Hydroxy-3',4',5',6'-fluorophenyl)-10,15,20-tris(pentafluorophenyl)-2/3-oxa-2/3-oxoporphyrin ( <b>14</b> , mixture of two lactone isomers) .....	17
Swern oxidation of 10,15,20-Tris(pentafluorophenyl)-5-(tetrafluorochromene-annulated) chlorin ( <b>6<sup>H</sup></b> ): .....	22
10,15,20-Tris(pentafluorophenyl)-5-(tetrafluorochromene-annulated)-3-methylthio-2-oxo-chlorin ( <b>15<sup>SCH<sub>3</sub></sup></b> ).....	22
[10,15,20-Tris(pentafluorophenyl)-5-(tetrafluorochromene-annulated)-2-oxo-3-yl]dimer ( <b>16</b> ).....	25
Dimer ( <b>17</b> ) .....	28
<b>NSD Analysis</b> .....	32
<b>Crystallographic Details</b> .....	35
General Procedures.....	35
Crystallographic Details for <b>16</b> .....	38
Crystallographic Details for <b>15<sup>SCH<sub>3</sub></sup></b> .....	39
Crystallographic Details for <b>14</b> .....	42

**CrO<sub>3</sub> Oxidation of 5,10,15,20-Tetrakis(pentafluorophenyl)-2,3-cis-dihydroxychlorin (2<sup>F</sup>)**

**5,10,15,20-Tetrakis(pentafluorophenylporpholactone 4<sup>F</sup> – Known compound,<sup>1</sup> included for reference**

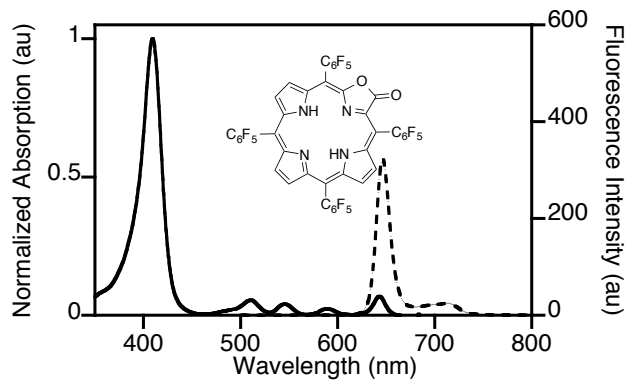


**Figure S1.** UV-Vis (black solid trace) and fluorescence (black dotted trace) spectra of **4<sup>F</sup>** ( $\text{CH}_2\text{Cl}_2$ );  $\lambda_{\text{excitation}} = \lambda_{\text{Soret}}$

---

1. (a) M. Gouterman, R. J. Hall, G. E. Khalil, P. C. Martin, E. G. Shankland, R. L. Cerny, *J. Am. Chem. Soc.* **1989**, *111*, 3702–3707. (b) Y. Yu, H. Lv, X. Ke, B. Yang, J.-L. Zhang, *Adv. Synth. Catal.* **2012**, *354*, 3509–3516. (c) C. Brückner, J. Ogikubo, J. R. McCarthy, J. Akhigbe, M. A. Hyland, P. Daddario, J. L. Worlinsky, M. Zeller, J. T. Engle, C. J. Ziegler, M. J. Ranaghan, M. N. Sandberg, R. R. Birge, *J. Org. Chem.* **2012**, *77*, 6480–6494.

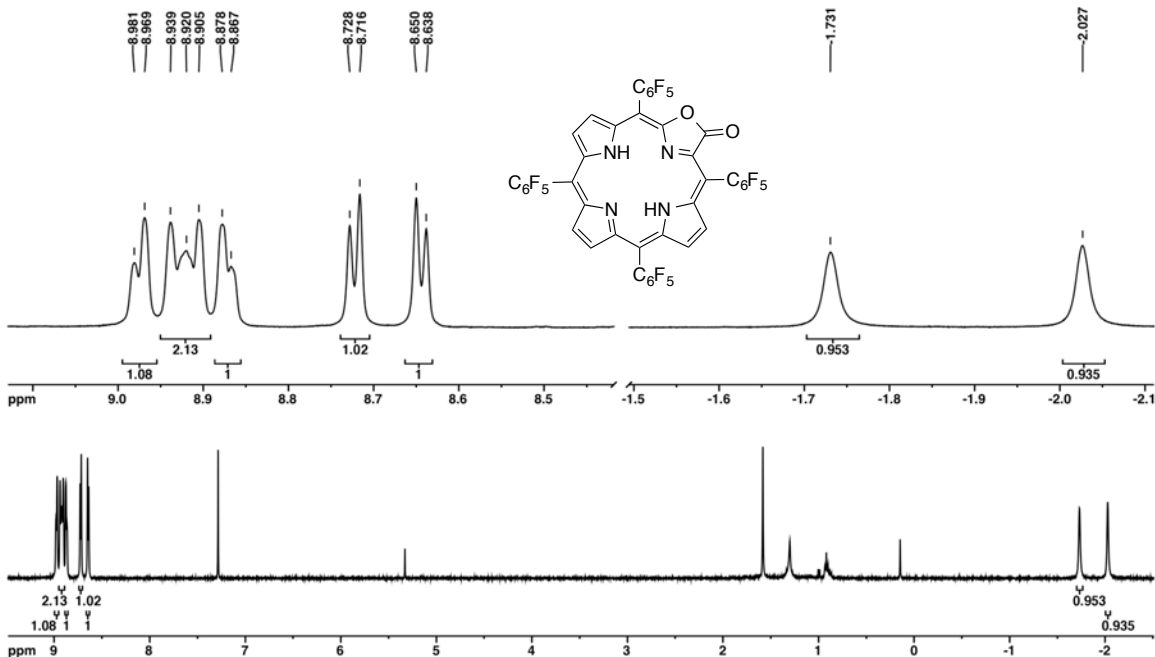


**Figure S2.**  $^1\text{H}$  NMR (400 MHz,  $\text{CDCl}_3$ ) spectrum of compound  $4^{\text{F}}$

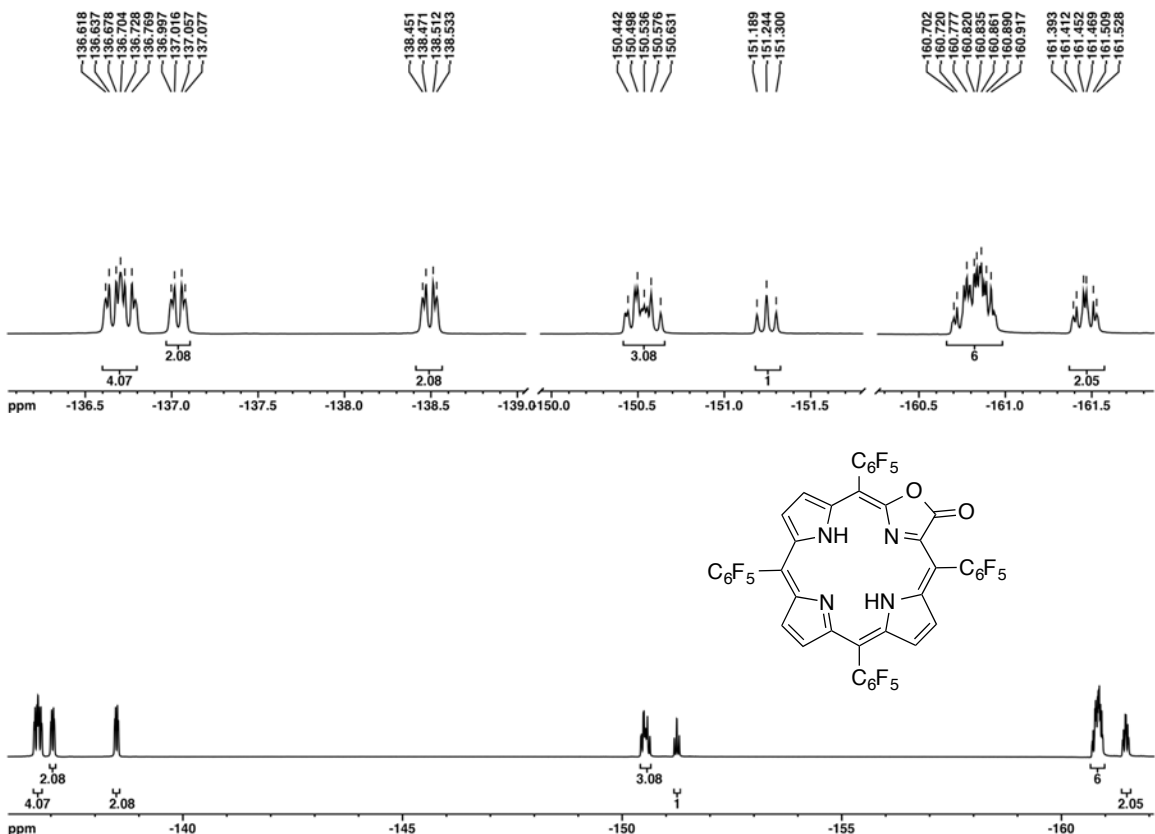


**Figure S3.**  $^{19}\text{F}$  NMR (376 MHz,  $\text{CDCl}_3$ ) spectrum of compound  $4^{\text{F}}$

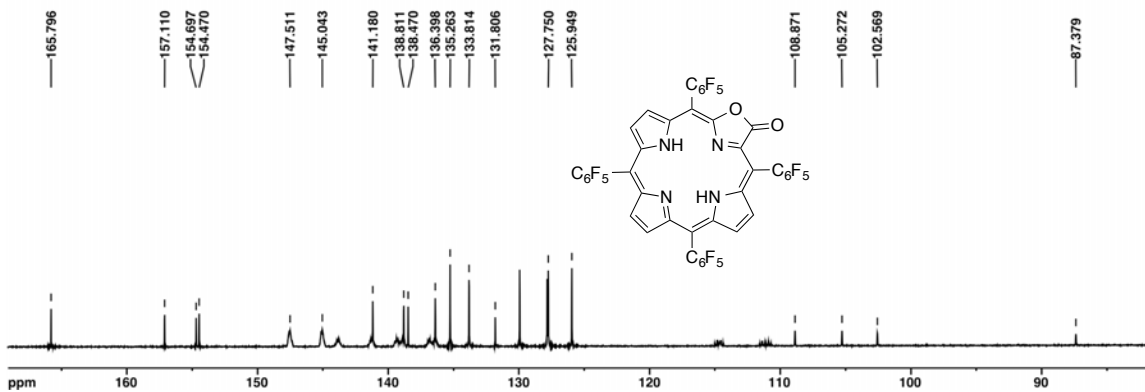


**Figure S4.**  $^{13}\text{C}$  NMR (100 MHz,  $\text{CDCl}_3$ ) spectrum of compound  $\mathbf{4}^{\text{F}}$

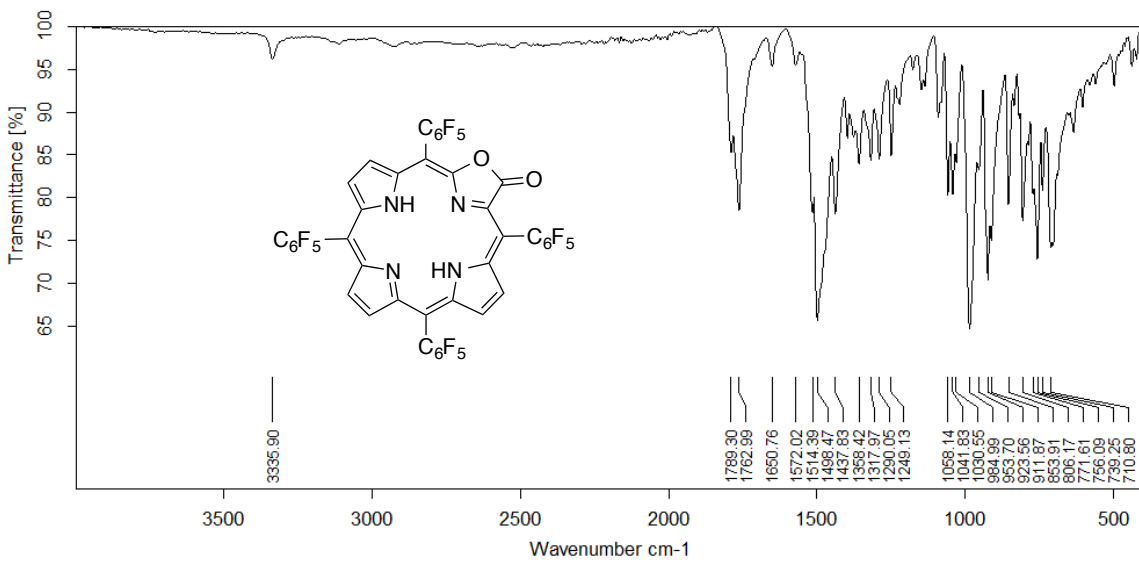


**Figure S5.** IR spectrum (neat, diamond ATR) of compound  $\mathbf{4}^{\text{F}}$

***meso*-Tetrakis(pentafluorophenyl)-2,3-dioxoporphyrin ( $3^F$ )**

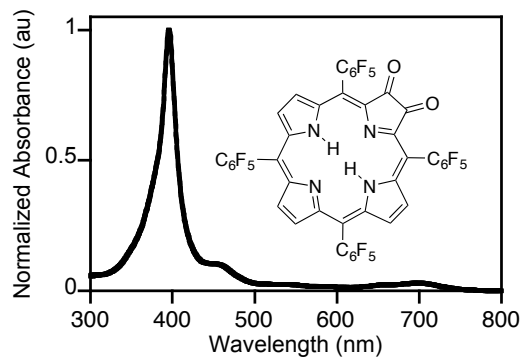


**Figure S6.** UV-Vis (black solid trace) spectrum of  $3^F$

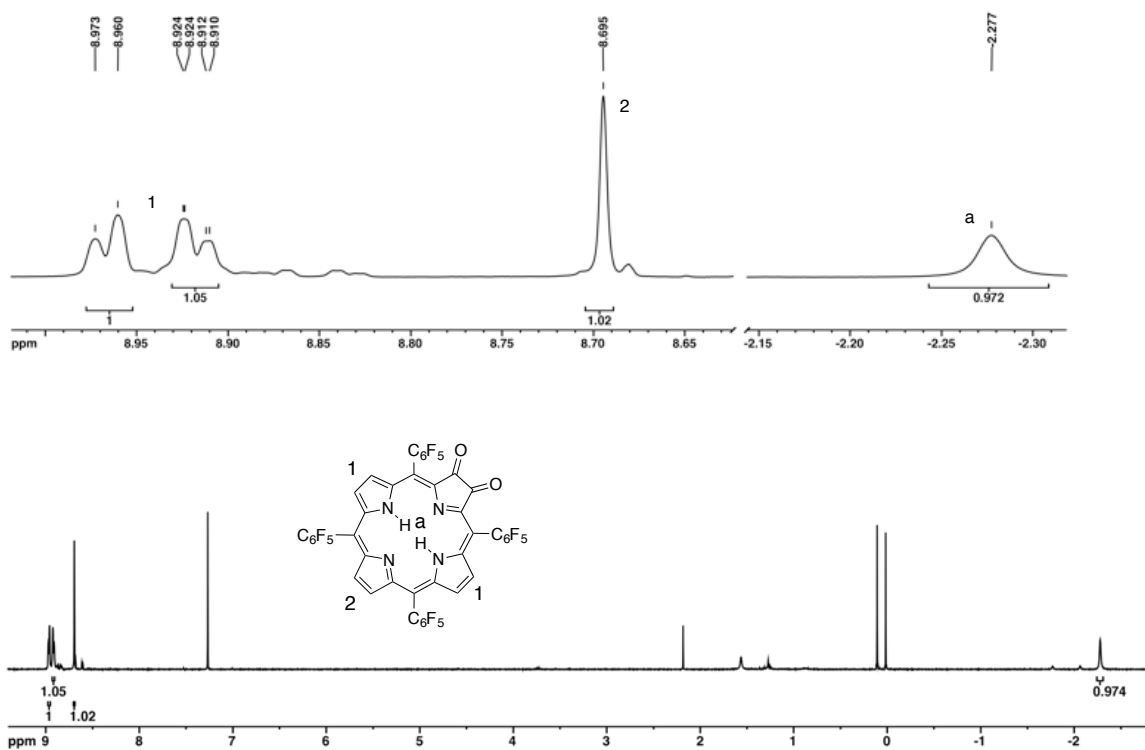


**Figure S7.** <sup>1</sup>H NMR (400 MHz, CDCl<sub>3</sub>) spectrum of compound  $3^F$

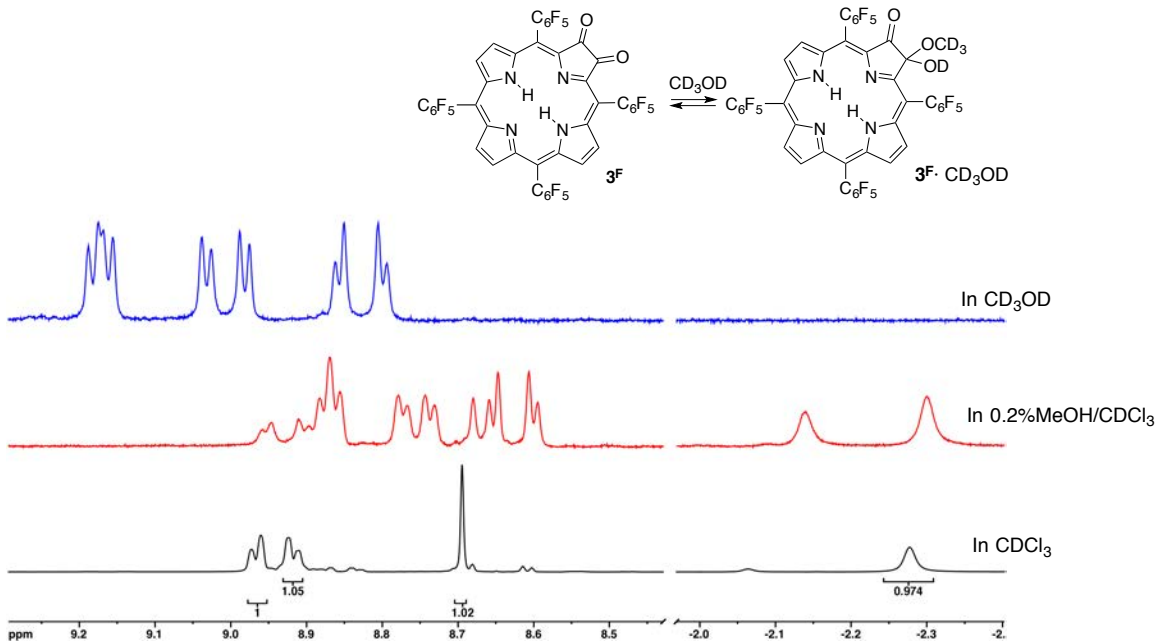


**Figure S8.**  $^1\text{H}$  NMR (400 MHz, black trace in  $\text{CDCl}_3$ , red trace in  $0.2\%\text{MeOH}/\text{CDCl}_3$  and blue trace in  $\text{CD}_3\text{OD}$ ) spectra of compound  $3\text{F}$

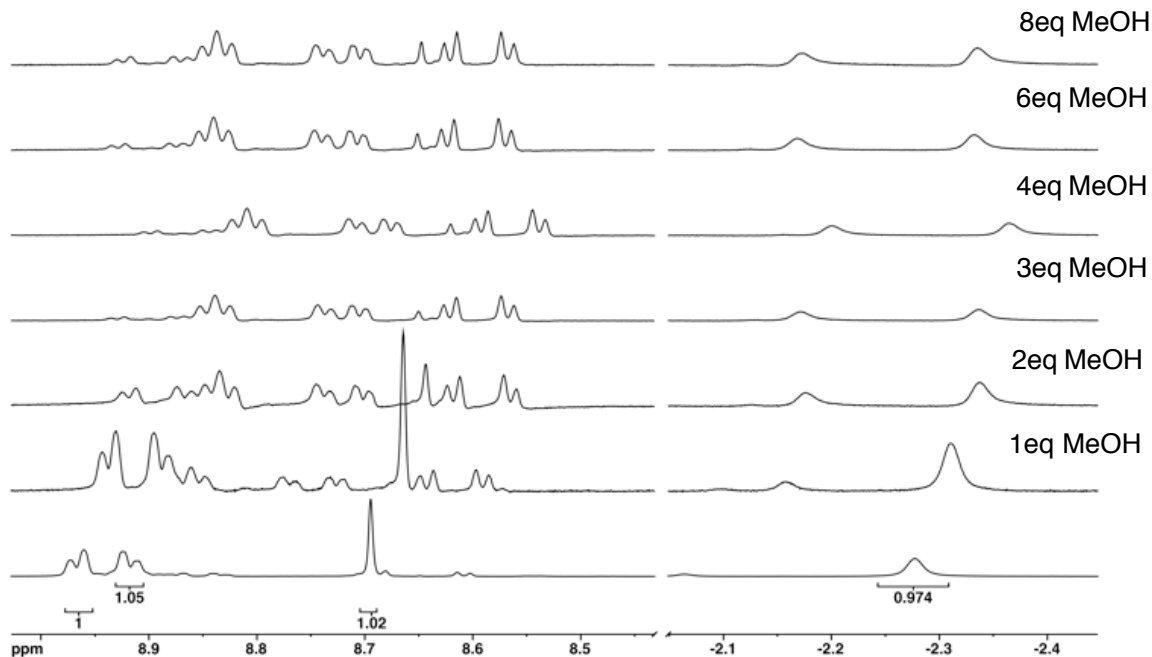


**Figure S9.**  $^1\text{H}$  NMR (400 MHz in  $\text{CDCl}_3$ ) titration spectra of compound  $3\text{F}$  with methanol

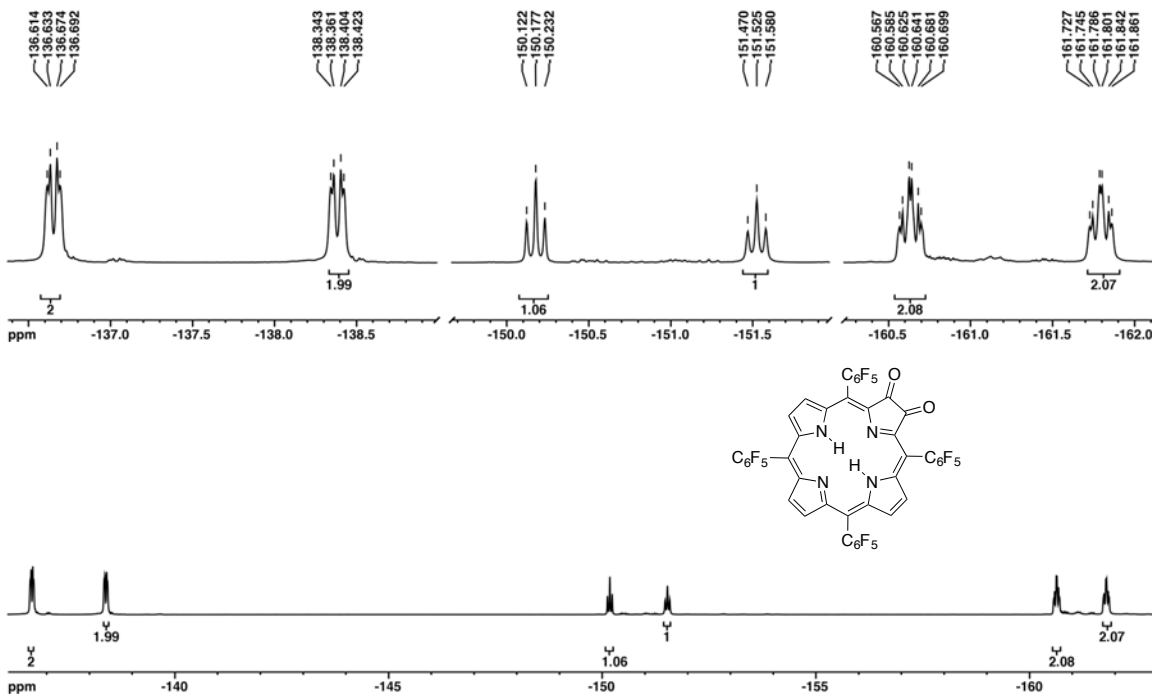


**Figure S10.**  $^{19}\text{F}$  NMR (376 MHz,  $\text{CDCl}_3$ ) spectrum of compound  $3^{\text{F}}$

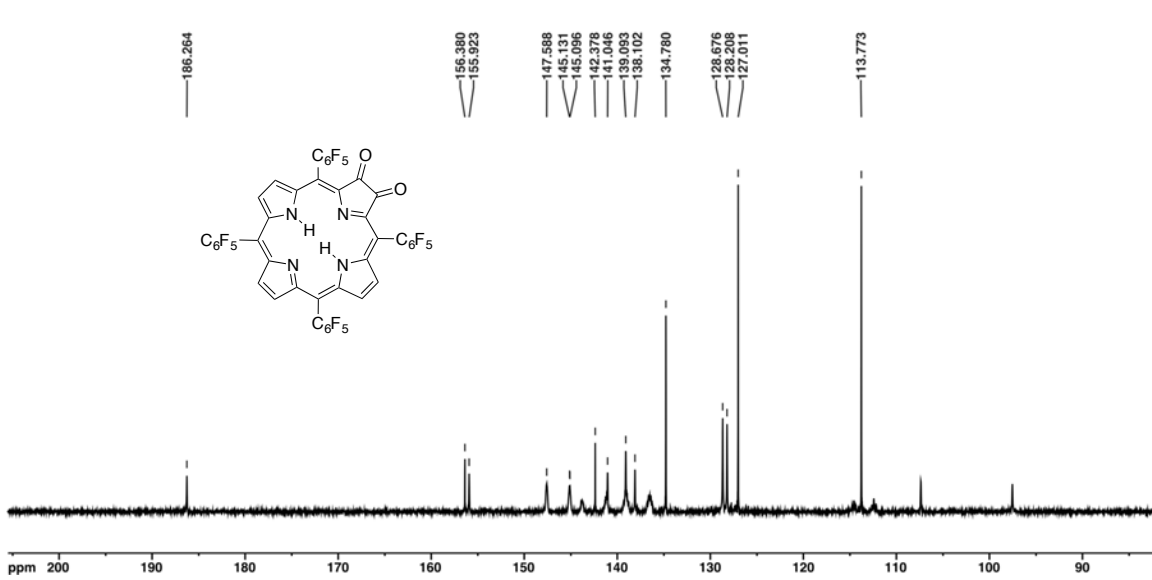


**Figure S11.**  $^{13}\text{C}$  NMR (100 MHz,  $\text{CDCl}_3$ ) spectrum of compound  $3^{\text{F}}$

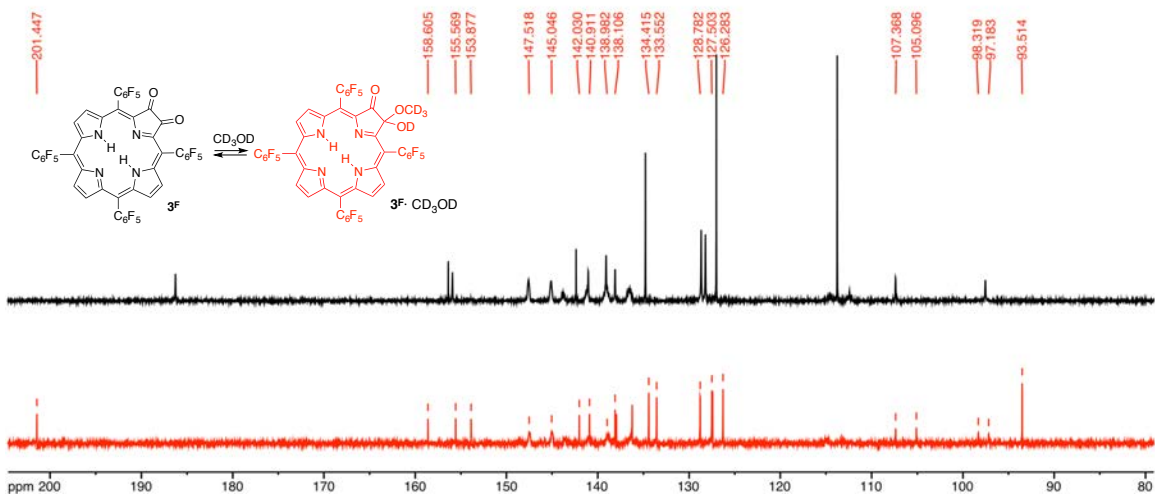


**Figure S12.**  $^{13}\text{C}$  NMR (100 MHz, black trace in  $\text{CDCl}_3$  at 300K, red trace in  $\text{CDCl}_3$  and 8 eq of MeOH at 280K) spectra of compound  $3^F$

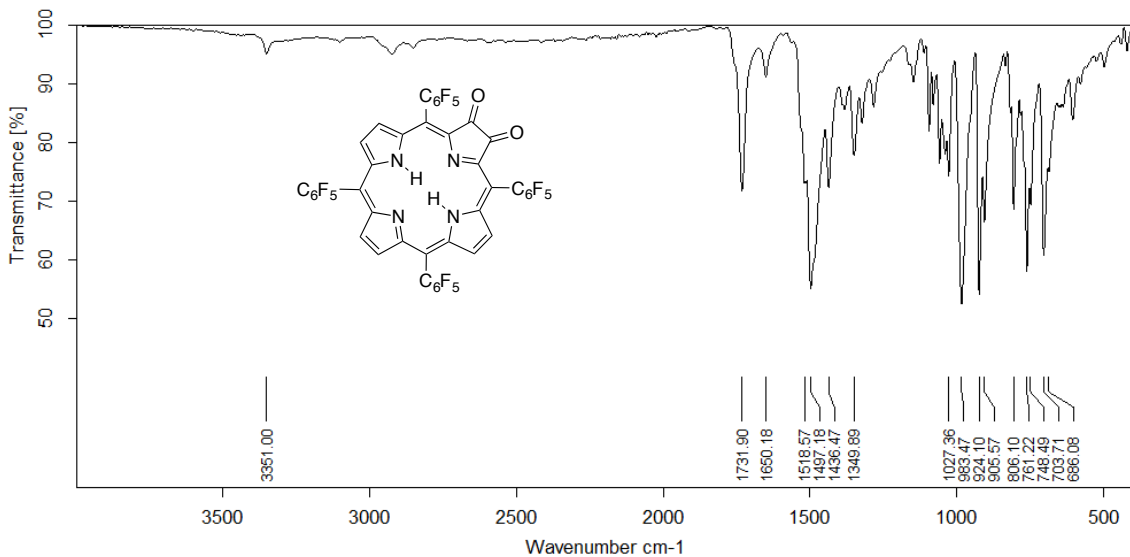


**Figure S13.** IR (neat, diamond ATR) spectrum of compound  $3^F$

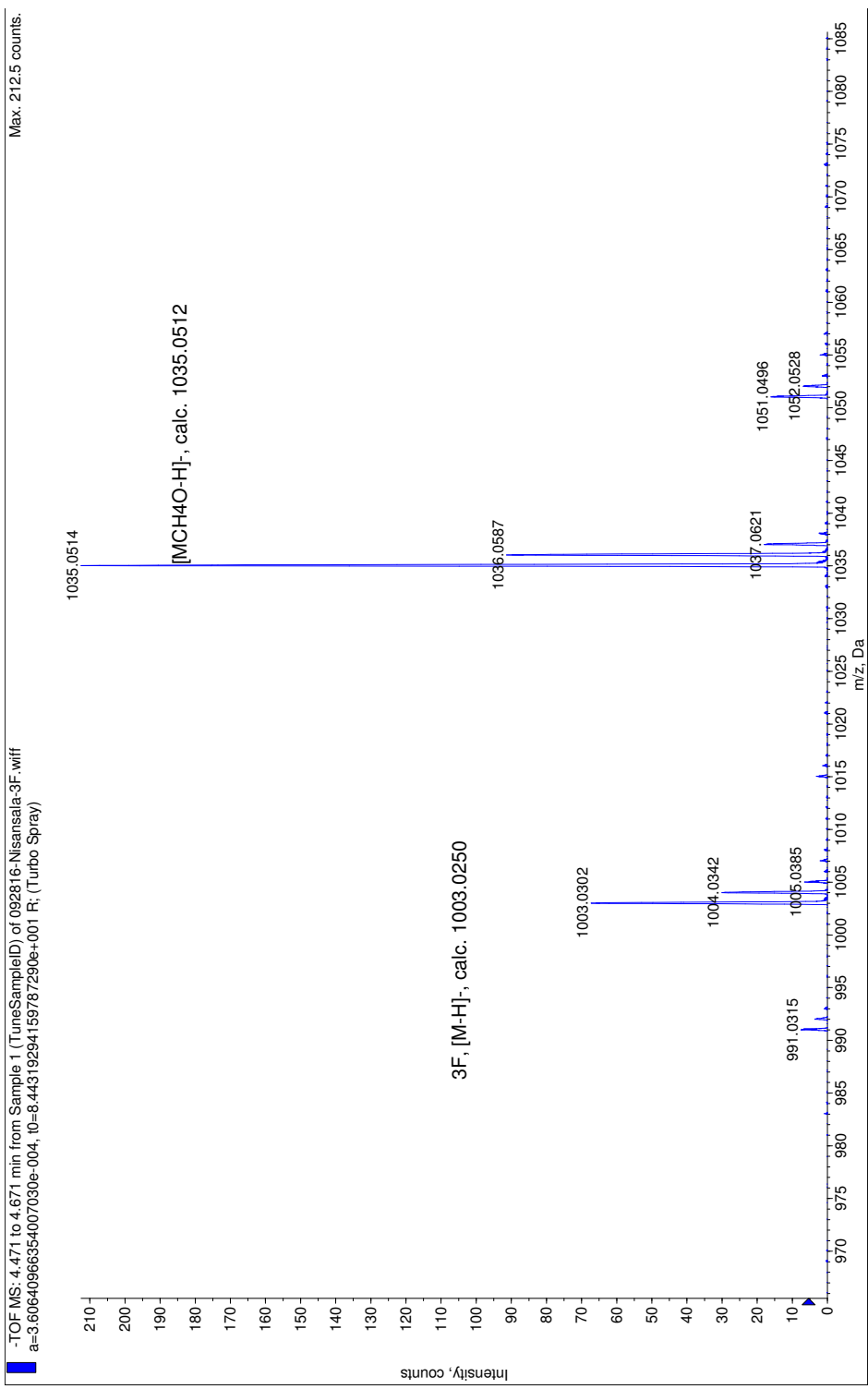


**Figure S14.** Mass spectrum (ESI-, 100% CH<sub>3</sub>OH, TOF) of 3<sup>F</sup>

**10,15,20-Tris(pentafluorophenyl)-5-(tetrafluorochromene-annulated)-3-hydroxy-2-oxo-chlorin ( $\mathbf{15}^{\text{OH}}$ )**

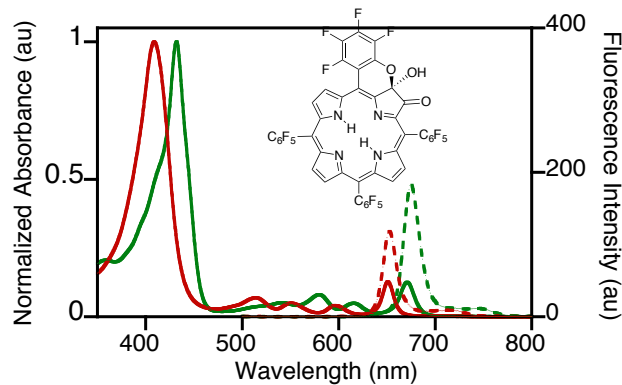


**Figure S15.** UV-Vis (green solid trace in  $\text{CH}_2\text{Cl}_2$  and red solid trace in  $\text{CH}_3\text{OH}$ ) and fluorescence (green dotted trace in  $\text{CH}_2\text{Cl}_2$  and red dotted trace in  $\text{CH}_3\text{OH}$ ) spectra of  $\mathbf{15}^{\text{OH}}$ ;  $\lambda_{\text{excitation}} = \lambda_{\text{Soret}}$

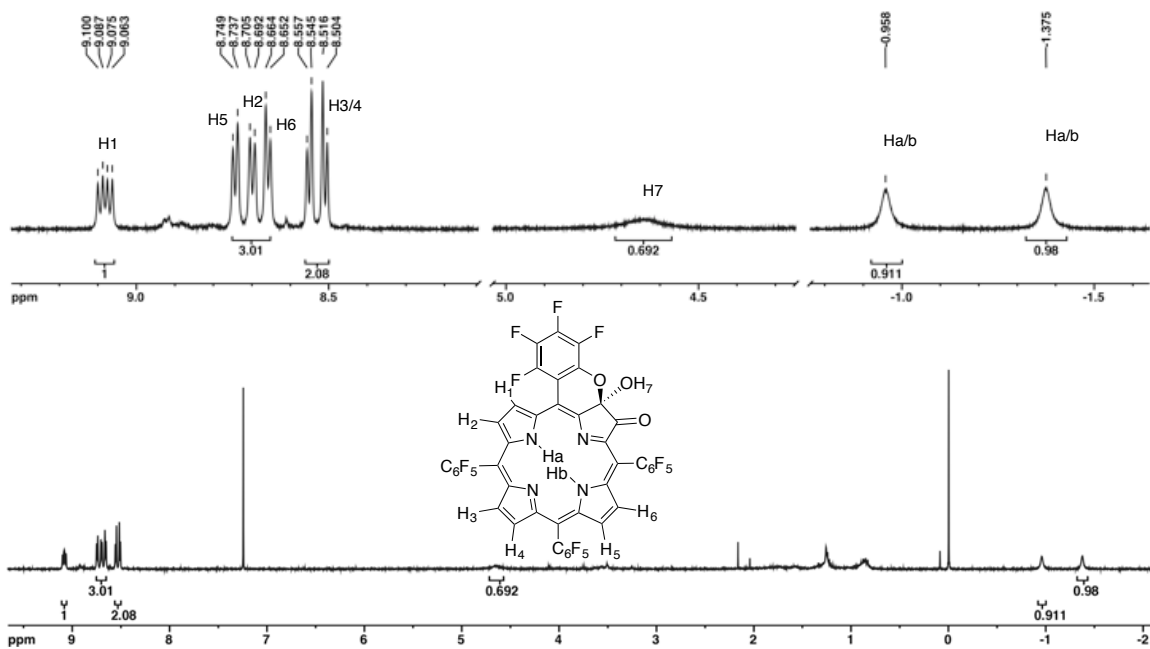


**Figure S16.**  ${}^1\text{H}$  NMR (400 MHz,  $\text{CDCl}_3$ ) spectrum of compound  $\mathbf{15}^{\text{OH}}$

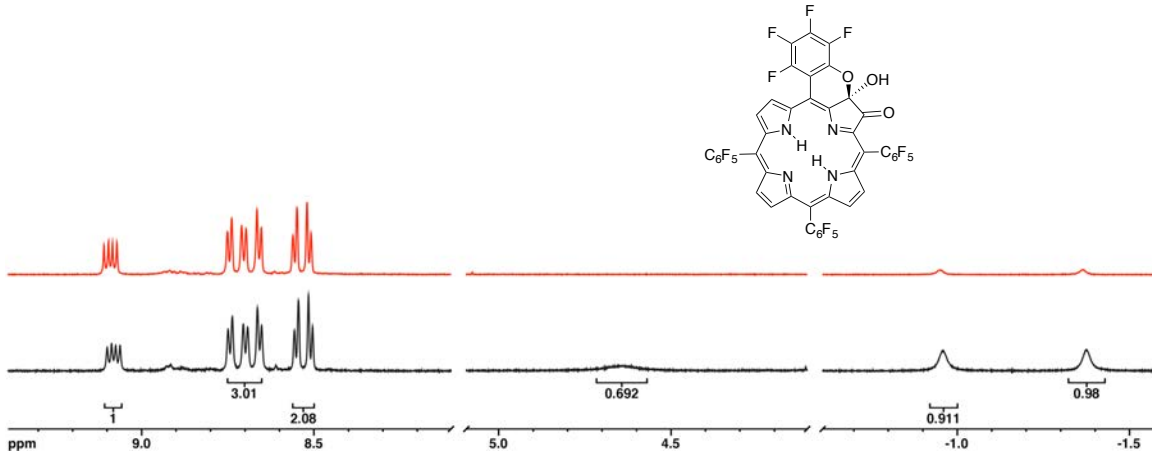


**Figure S17.**  $\text{D}_2\text{O}$  exchange  $^1\text{H}$  NMR (400 MHz,  $\text{CDCl}_3$ ) of compound  $15^{\text{OH}}$ , black solid trace before  $\text{D}_2\text{O}$ , red solid trace after  $\text{D}_2\text{O}$  exchange

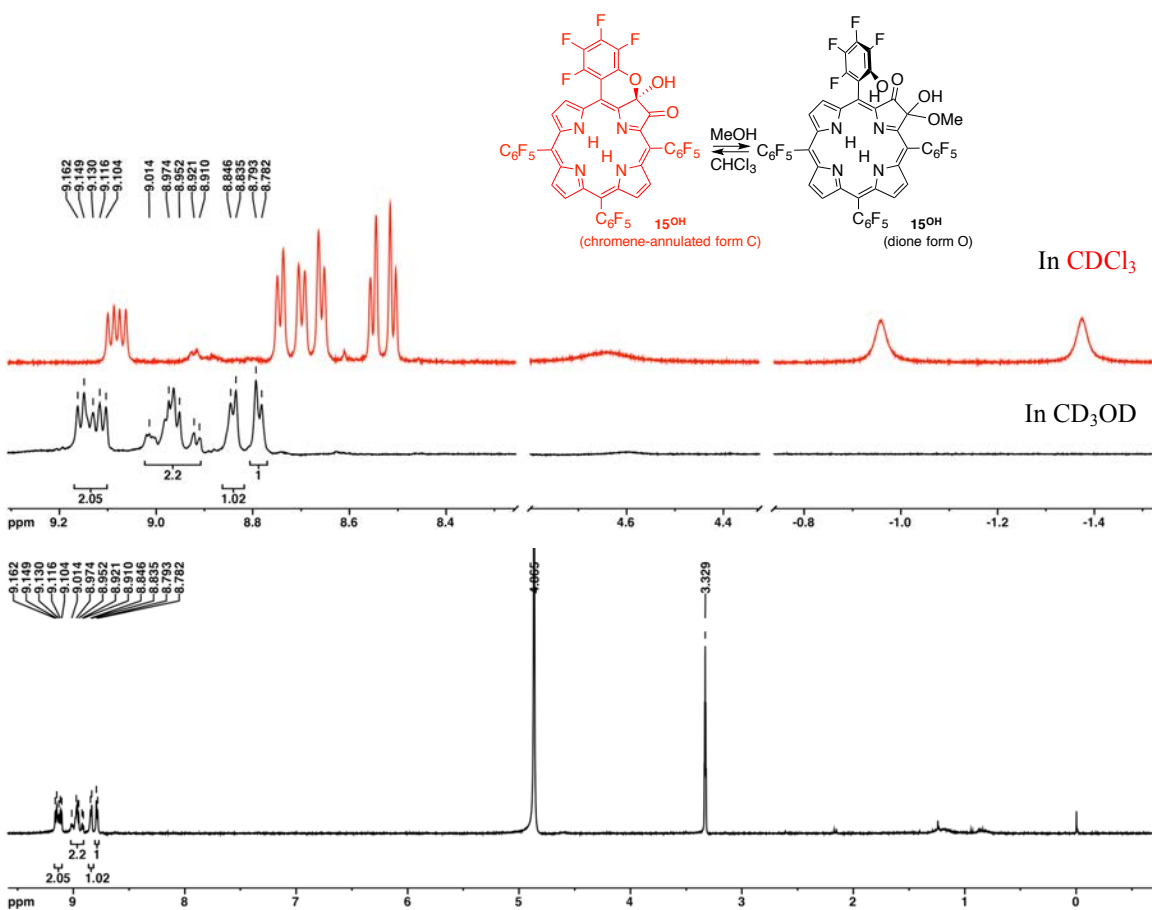


**Figure S18.**  $^1\text{H}$  NMR (400 MHz) spectra of compound  $15^{\text{OH}}$ , black solid trace in  $\text{CD}_3\text{OD}$ , red solid trace in  $\text{CDCl}_3$

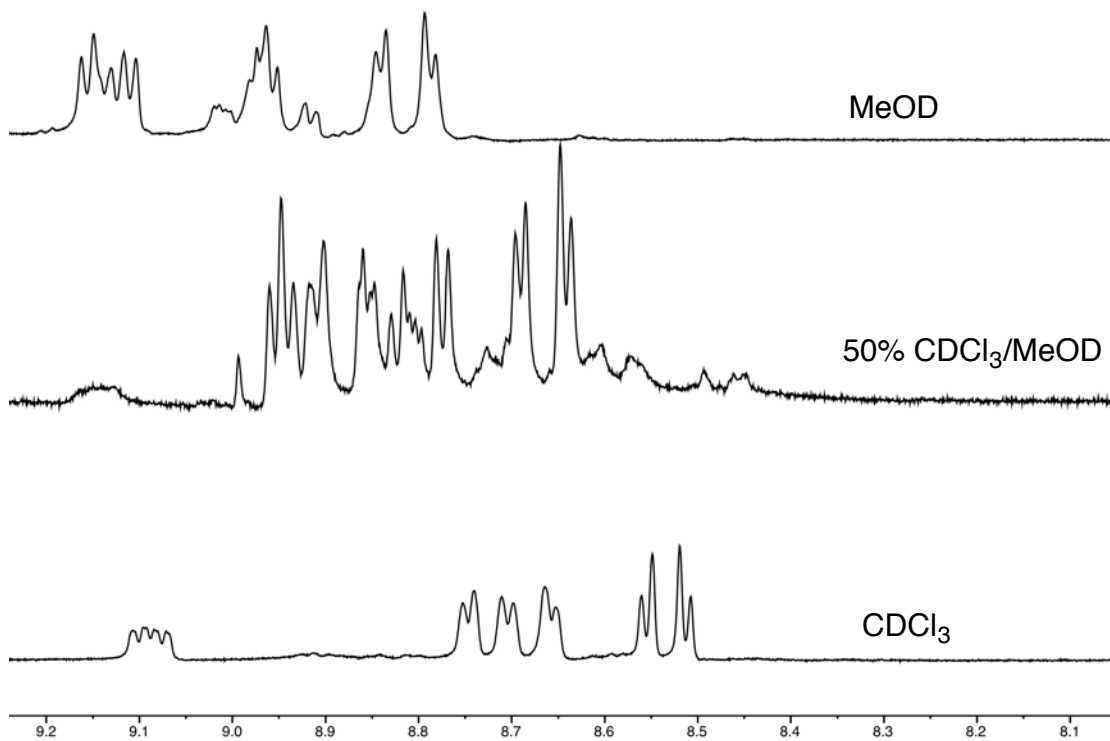


**Figure S19.**  $^1\text{H}$  NMR (400 MHz) spectra of compound  $\mathbf{15}^{\text{OH}}$  at 280K.

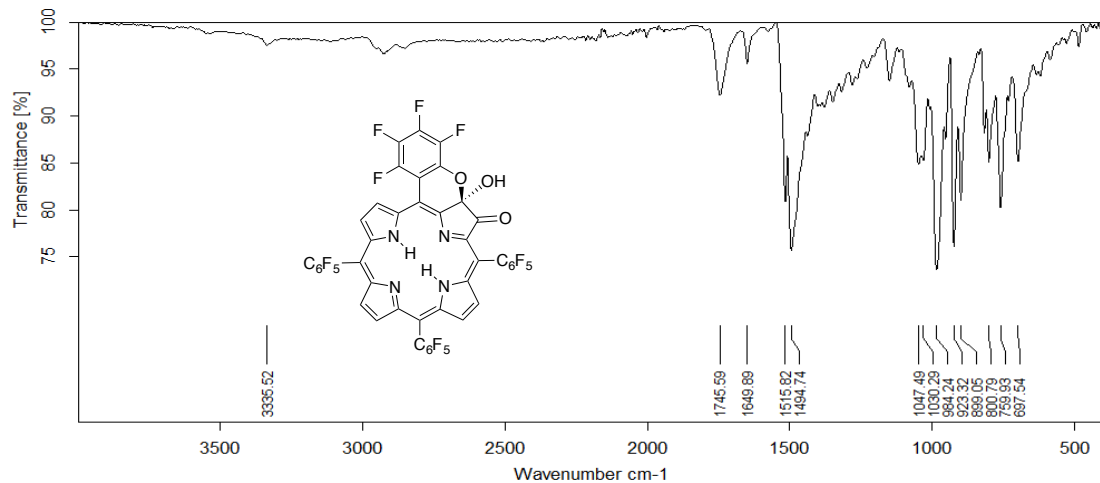


**Figure S20.** IR (neat, diamond ATR) spectrum of compound  $\mathbf{15}^{\text{OH}}$

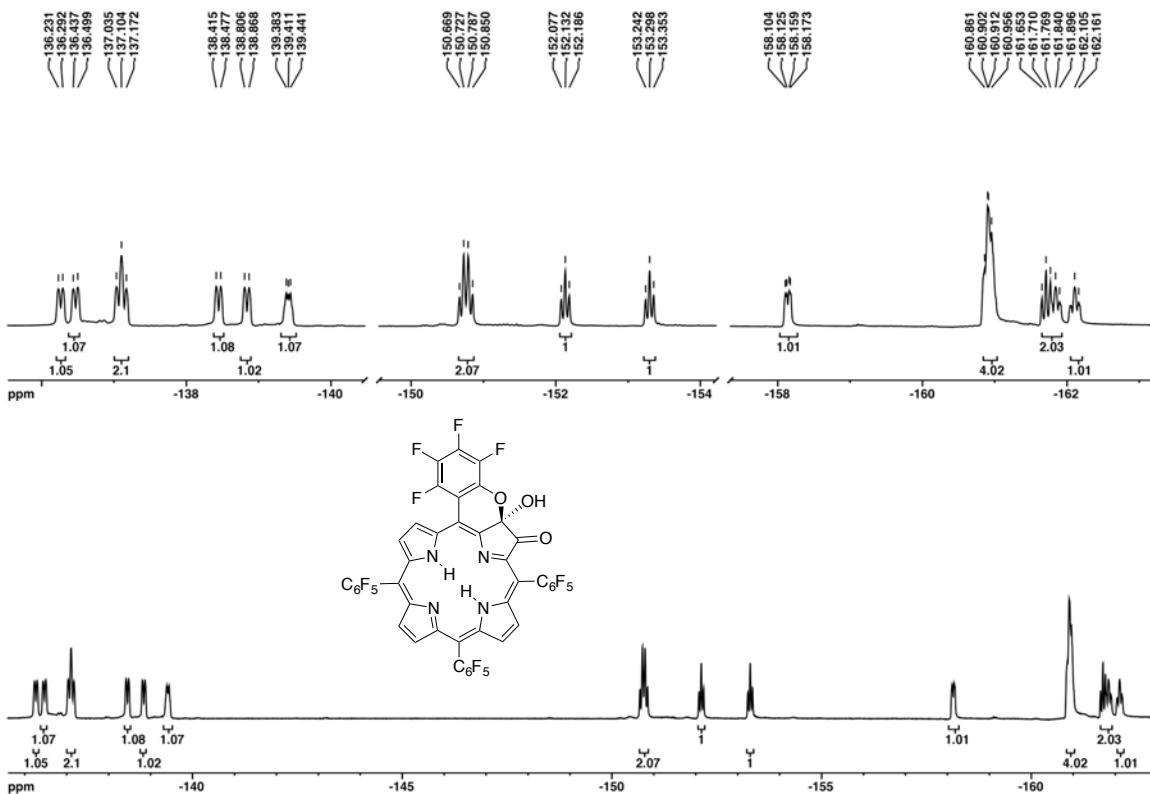


**Figure S21.**  $^{19}\text{F}$  NMR (376 MHz,  $\text{CDCl}_3$ ) spectrum of compound  $\mathbf{15}^{\text{OH}}$

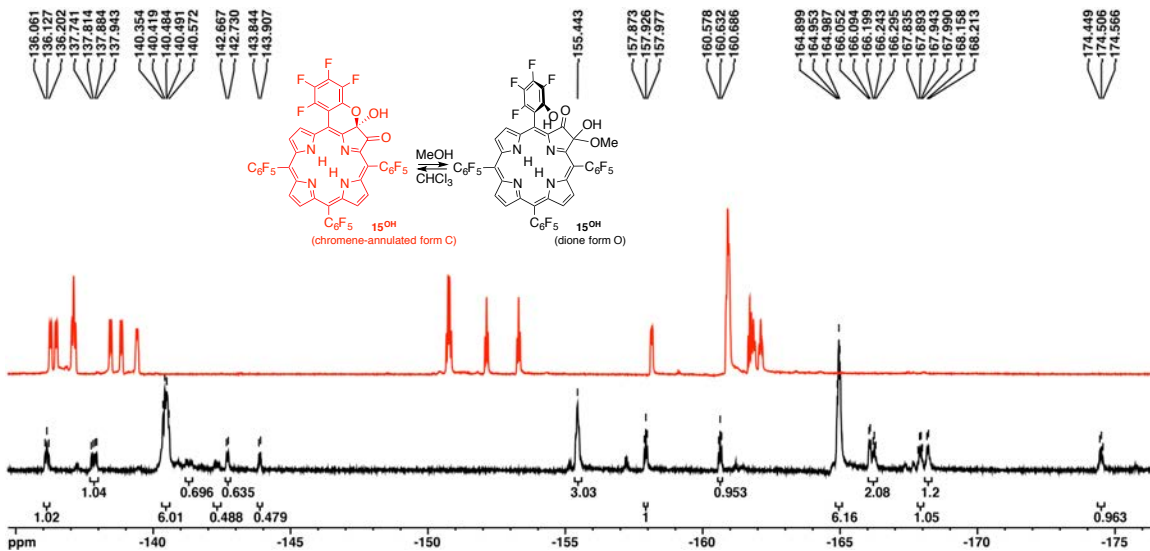


**Figure S22.**  $^{19}\text{F}$  NMR (376 MHz, red trace in  $\text{CDCl}_3$ , black trace in  $\text{CD}_3\text{OD}$ ) spectrum of compound  $\mathbf{15}^{\text{OH}}$

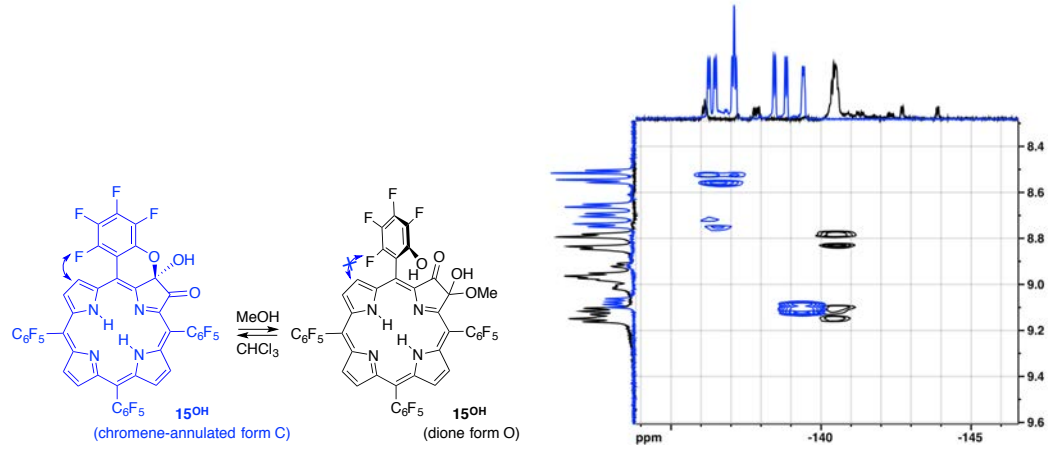


**Figure S23.** <sup>1</sup>H-<sup>19</sup>F COSY NMR (376 MHz, blue trace in CDCl<sub>3</sub>, black trace in CD<sub>3</sub>OD) spectrum of compound **15<sup>OH</sup>**

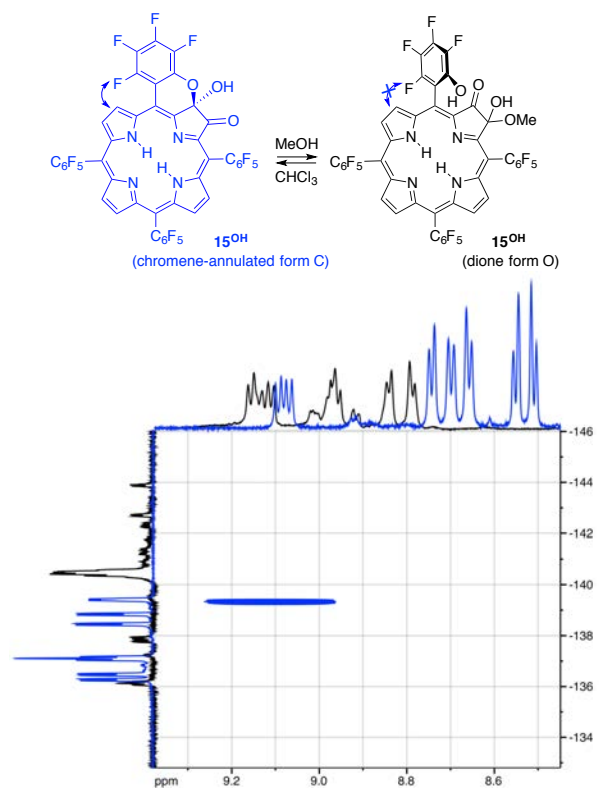


**Figure S24.** <sup>19</sup>F-<sup>1</sup>H COSY NMR (376 MHz, blue trace in CDCl<sub>3</sub>, black trace in CD<sub>3</sub>OD) spectrum of compound **15<sup>OH</sup>**

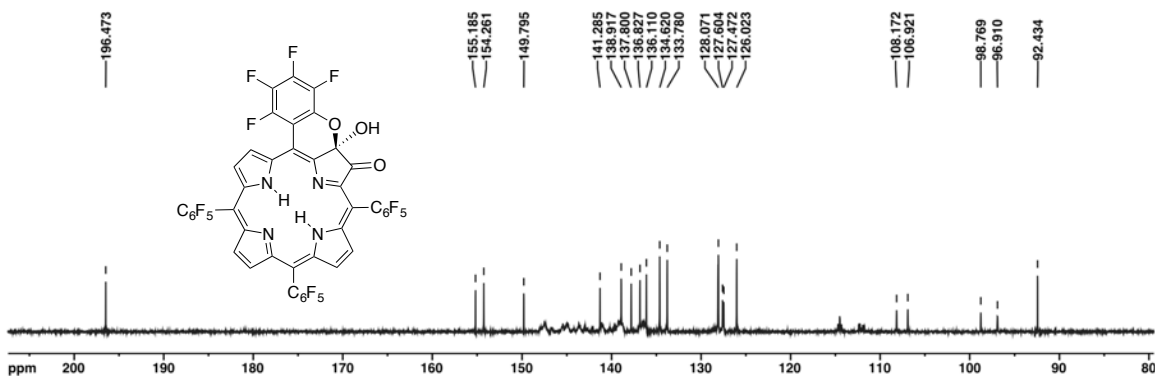


**Figure S25.**  $^{13}\text{C}$  NMR (100 MHz,  $\text{CDCl}_3$ ) spectrum of compound  $\mathbf{15}^{\text{OH}}$

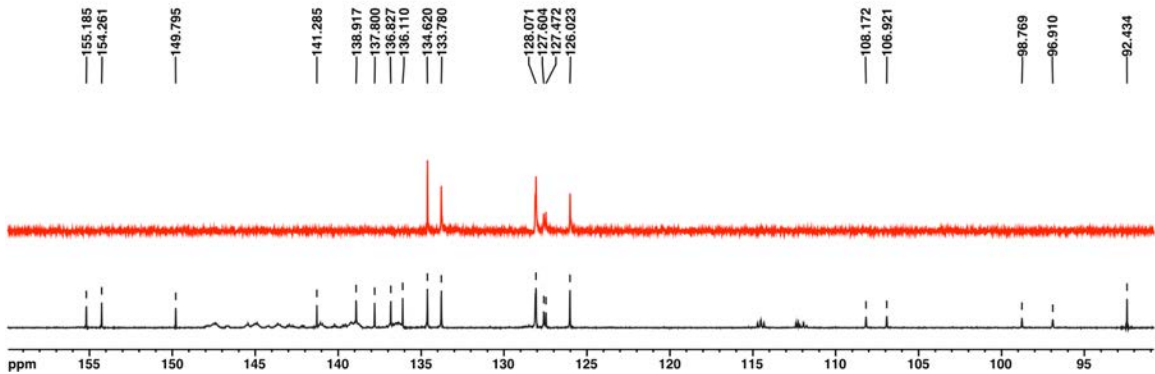


**Figure S26.**  $^{13}\text{C}$  NMR (black trace) and DEPT-135 (red trace) (100 MHz,  $\text{CDCl}_3$ ) of compound  $\mathbf{15}^{\text{OH}}$

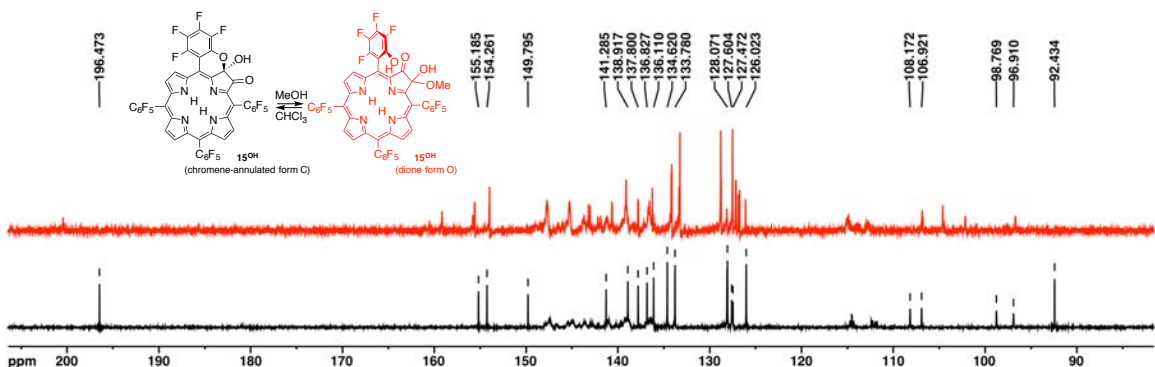


**Figure S27.**  $^{13}\text{C}$  NMR (100 MHz, black trace in  $\text{CDCl}_3$ , red trace in  $\text{CD}_3\text{OD}$ ) of compound  $\mathbf{15}^{\text{OH}}$

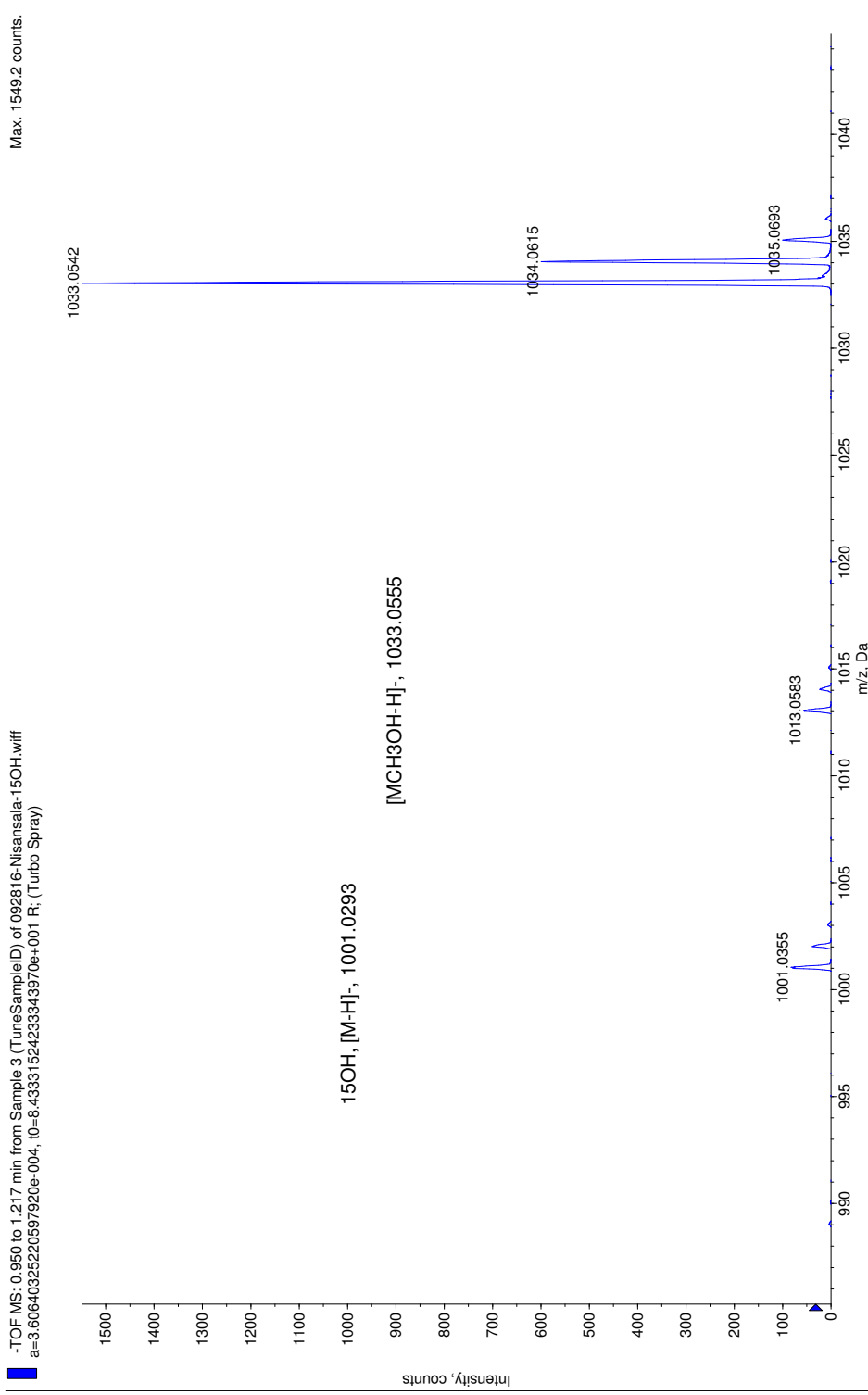


**Figure S28.** Mass spectrum (ESI-, 100% CH<sub>3</sub>OH, TOF) of **15<sup>OH</sup>**

**5-(2'-Hydroxy-3',4',5',6'-fluorophenyl)-10,15,20-tris(pentafluorophenyl)-2/3-oxa-2/3-oxoporphyrin (14, mixture of two lactone isomers)**

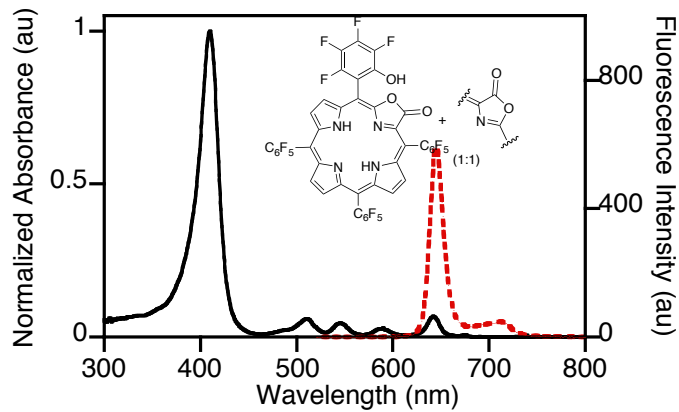


**Figure S29.** UV-Vis (black solid trace) and fluorescence (red dotted trace) spectra of **14** (1:1 mixture of two isomers) ( $\text{CH}_2\text{Cl}_2$ );  $\lambda_{\text{excitation}} = \lambda_{\text{Soret}}$

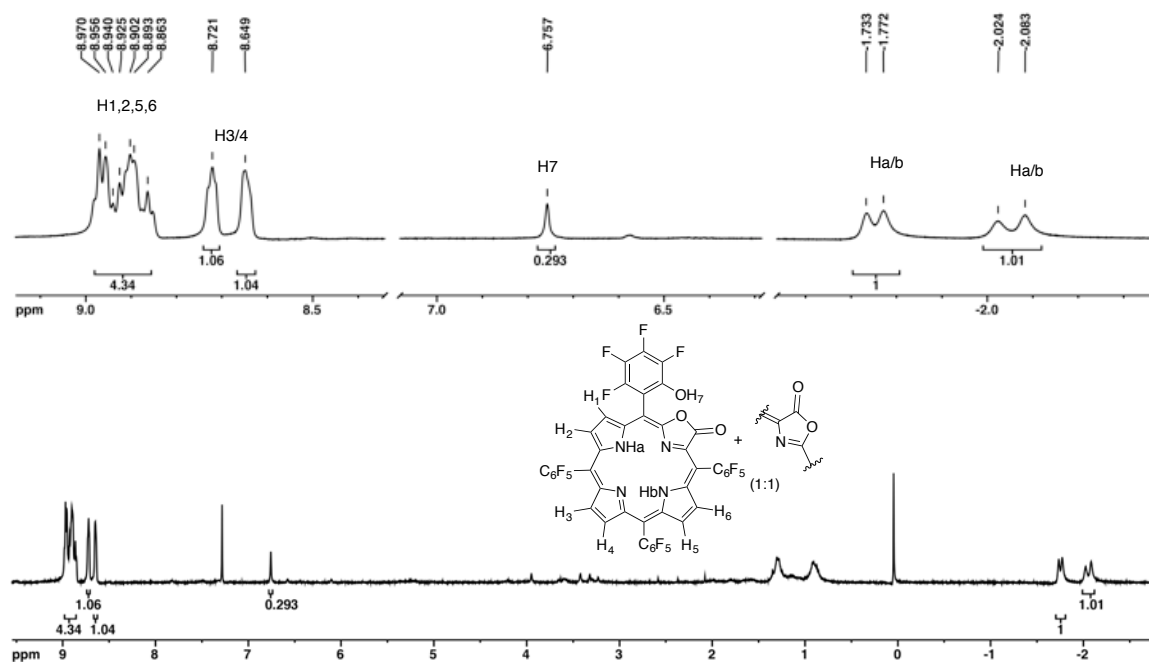


**Figure S30.**  $^1\text{H}$  NMR (400 MHz,  $\text{CDCl}_3$ ) spectrum of compound **14** (1:1 mixture of two isomers)

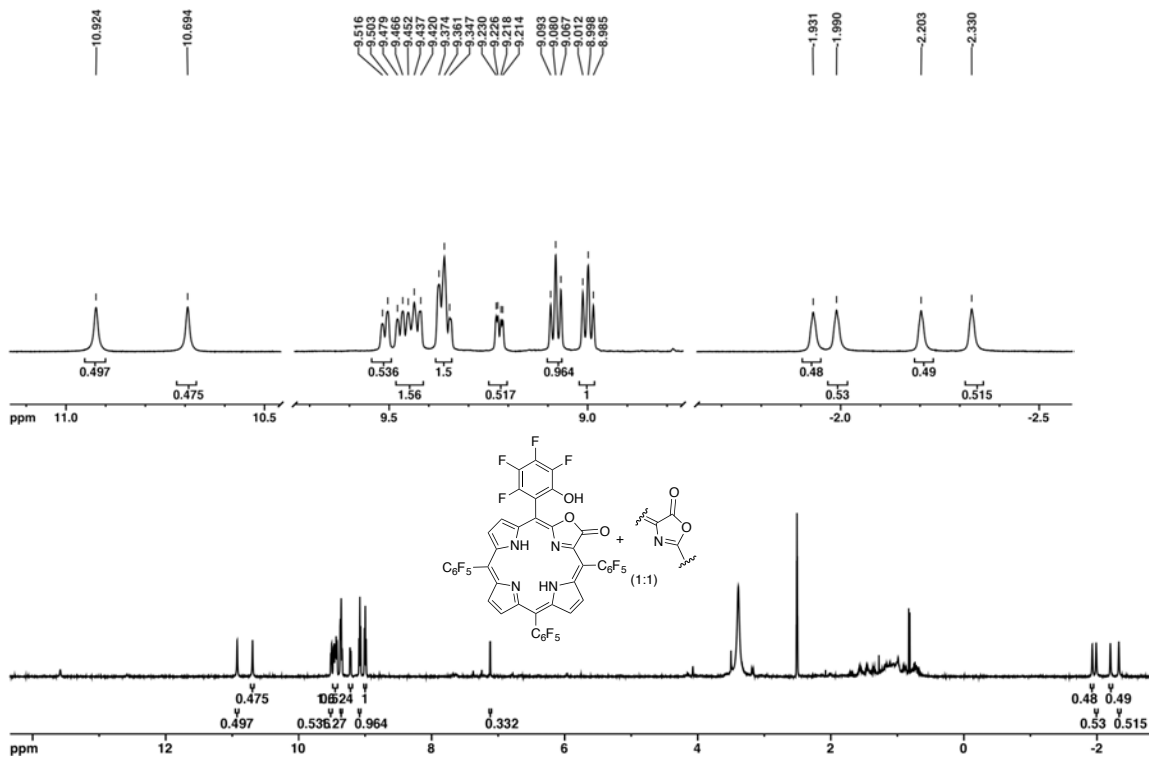


**Figure S31.**  $^1\text{H}$  NMR (400 MHz, DMSO-d<sub>6</sub>) spectrum of compound **14** (1:1 mixture of two isomers)

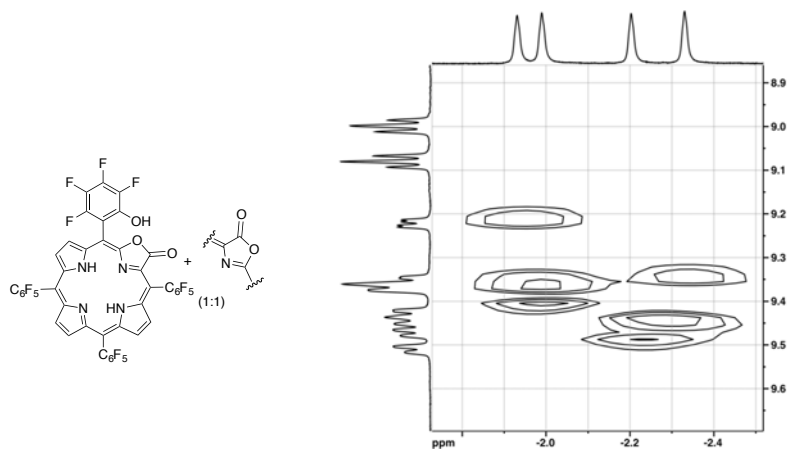


**Figure S32.**  $^1\text{H}$ - $^1\text{H}$  COSY NMR (400 MHz, DMSO-d<sub>6</sub>) spectrum of compound **14** (1:1 mixture of two isomers)

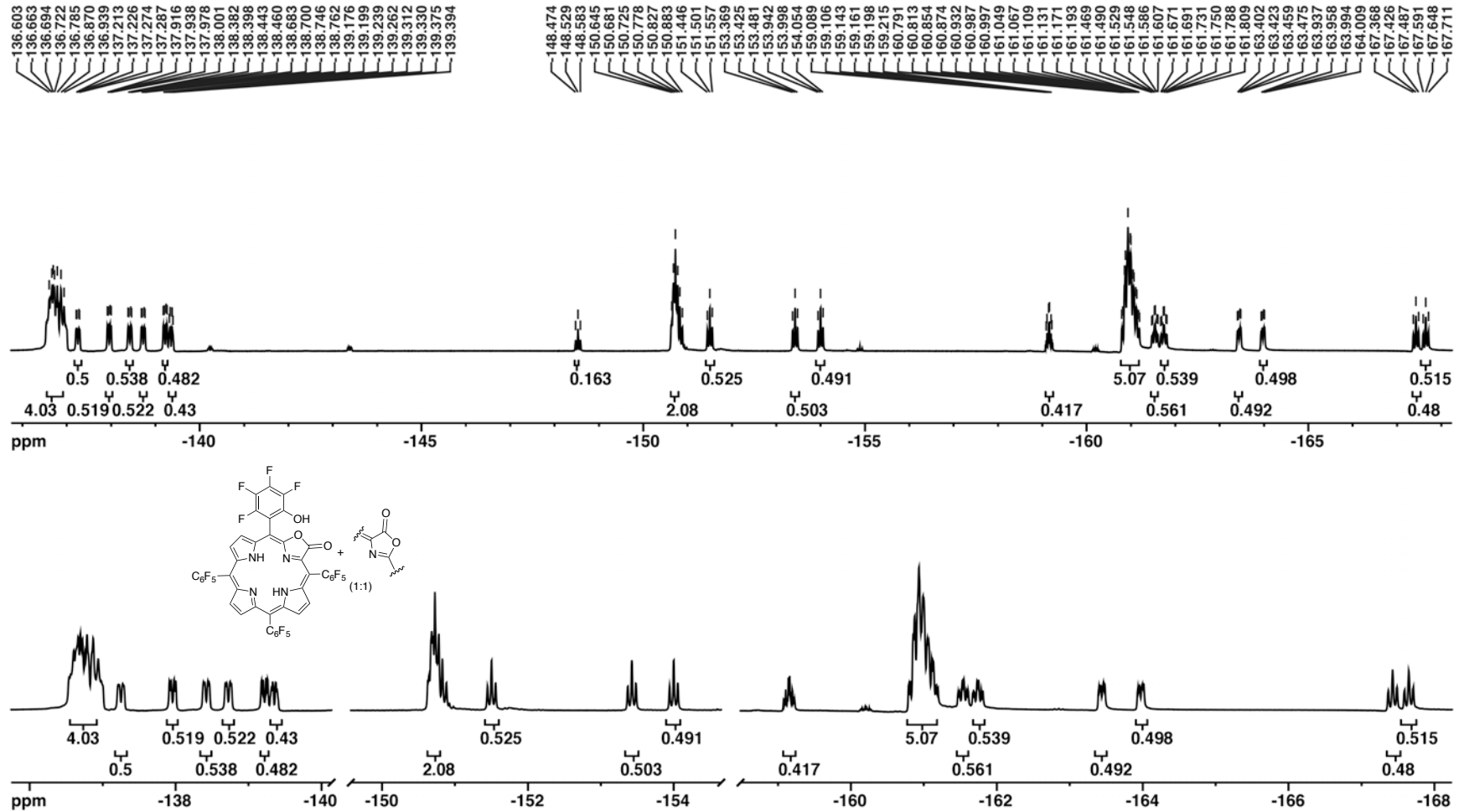
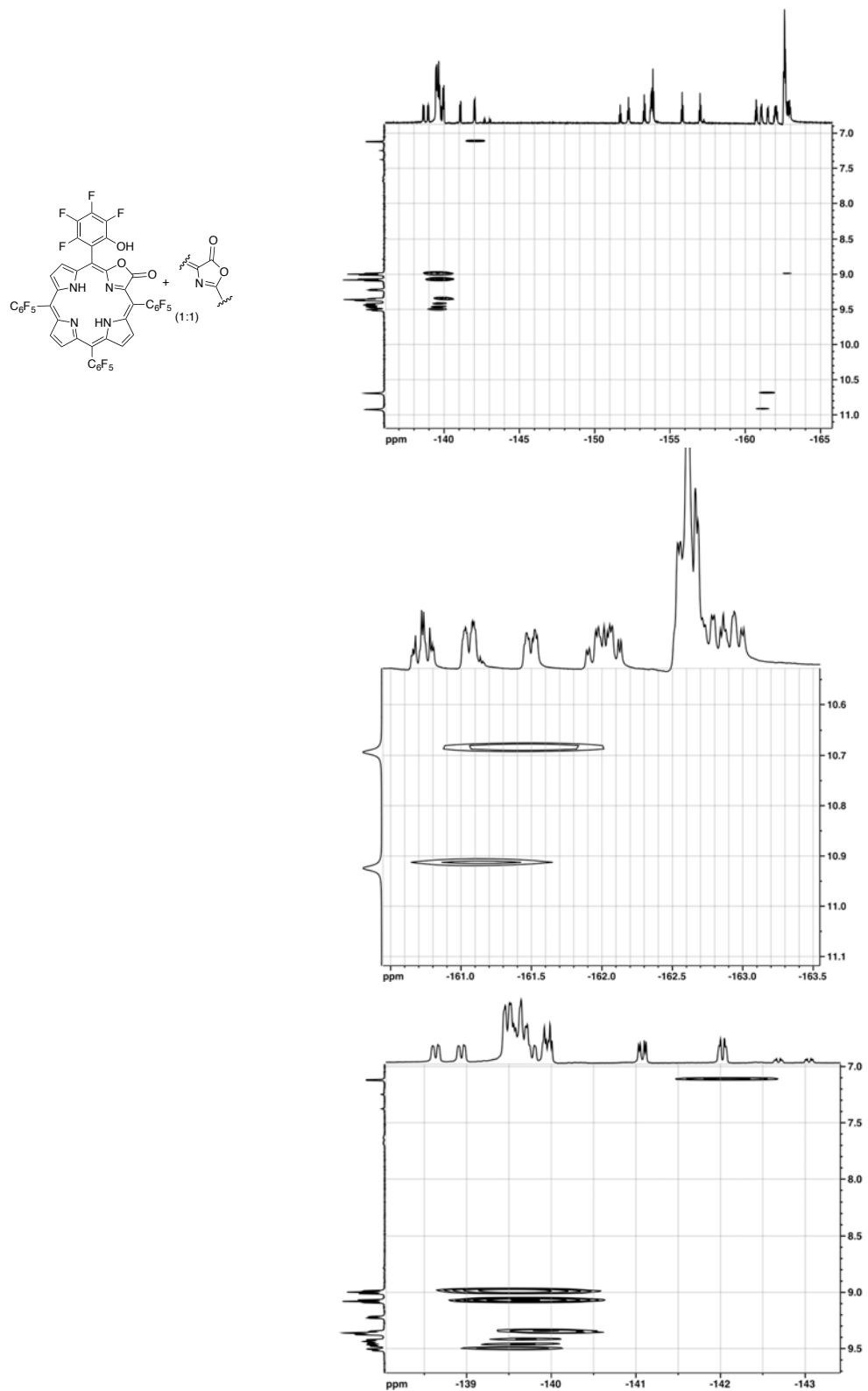
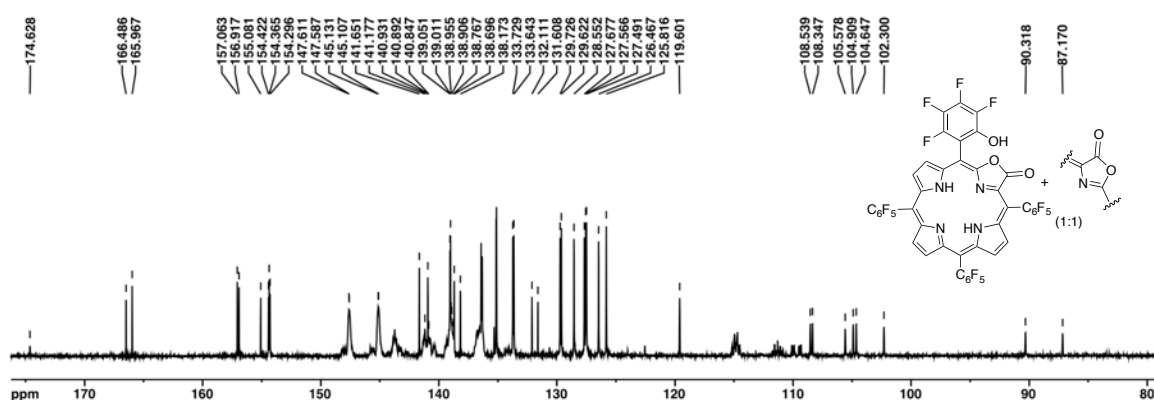


Figure S33. <sup>19</sup>F NMR (376MHz, CDCl<sub>3</sub>) spectrum of compound 14 (1:1 mixture of two isomers)



**Figure S34.** <sup>1</sup>H-<sup>19</sup>F COSY NMR (376 MHz, DMSO-d<sub>6</sub>) spectra of compound 14 (1:1 mixture of two isomers) at varying magnification



**Figure S35.** <sup>13</sup>C NMR (100 MHz, CDCl<sub>3</sub>) spectrum of compound **14**

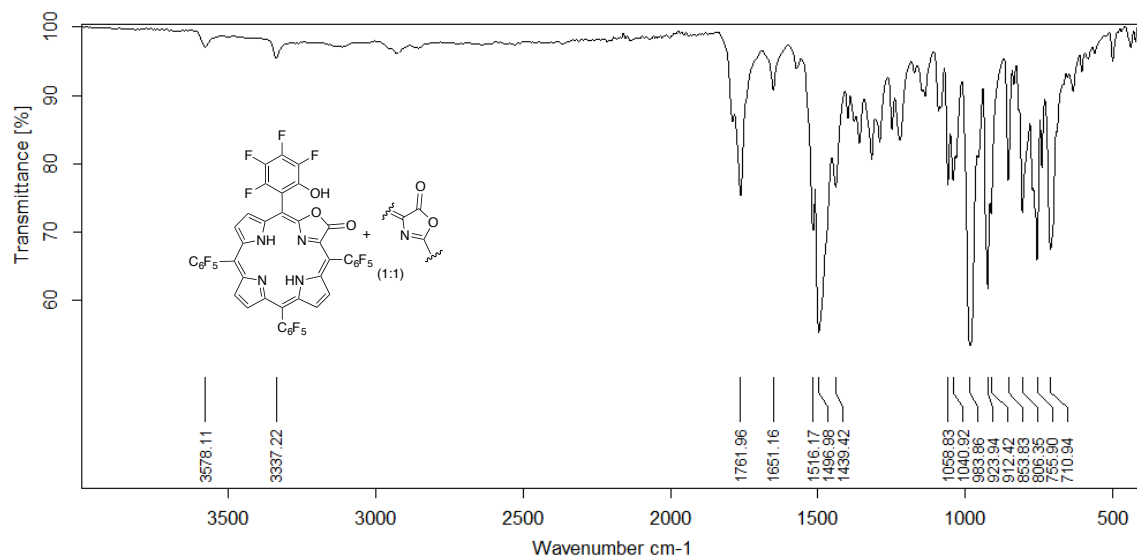


**Figure S36.** IR (neat, diamond ATR) spectrum of compound **14**

**Swern oxidation of 10,15,20-Tris(pentafluorophenyl)-5-(tetrafluorochromene-annulated) chlorin (**6<sup>H</sup>**):**

**10,15,20-Tris(pentafluorophenyl)-5-(tetrafluorochromene-annulated)-3-methylthio-2-oxo-chlorin (**15<sup>SCH<sub>3</sub></sup>****)

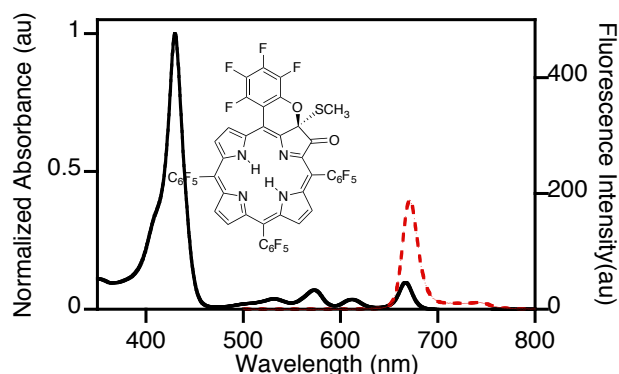


**Figure S37.** UV-Vis (black solid trace) and fluorescence (red dotted trace) spectra of **15<sup>SCH<sub>3</sub></sup>** ( $\text{CH}_2\text{Cl}_2$ );  $\lambda_{\text{excitation}} = \lambda_{\text{Soret}}$

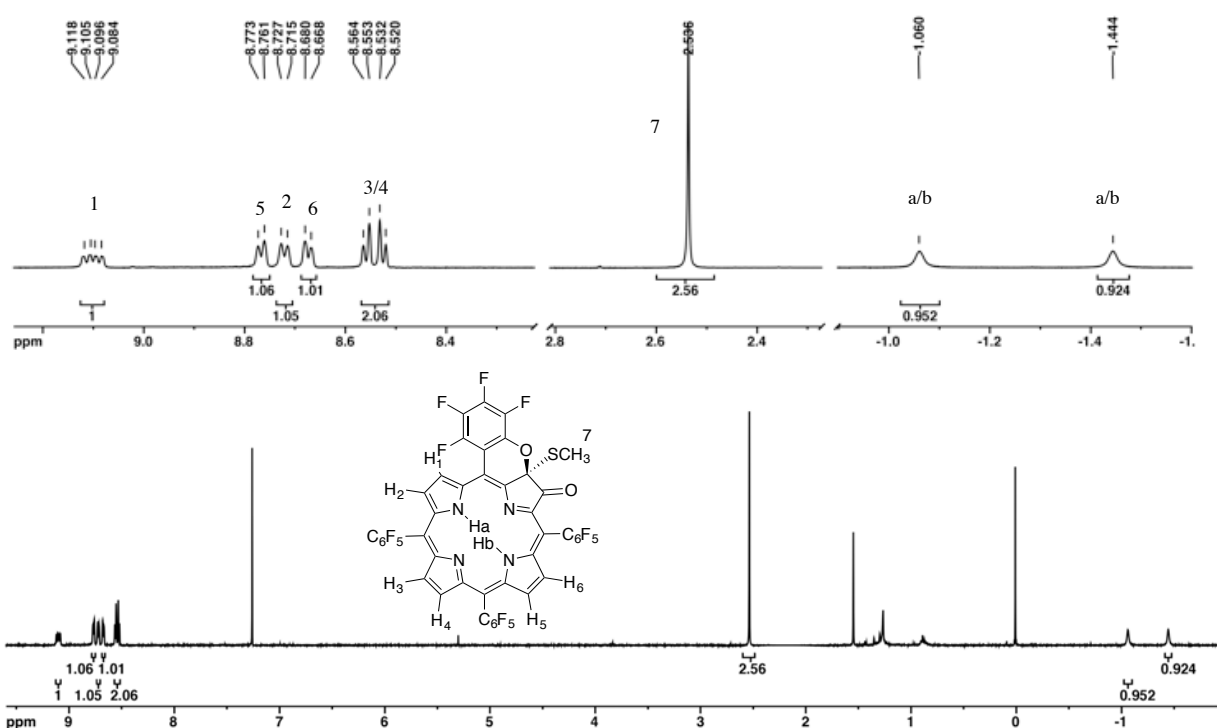


**Figure S38.** <sup>1</sup>H NMR (400 MHz,  $\text{CDCl}_3$ ) spectrum of compound **15<sup>SCH<sub>3</sub></sup>**

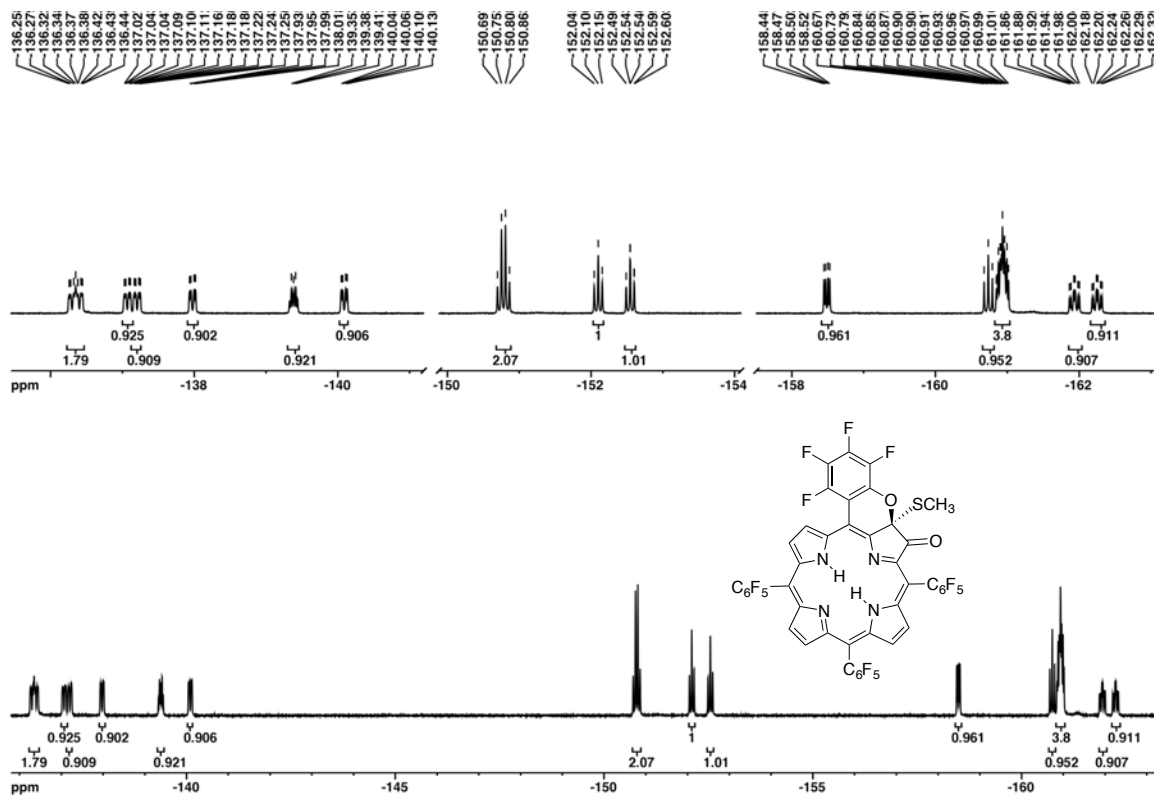


**Figure S39.**  $^{19}\text{F}$  NMR (376 MHz,  $\text{CDCl}_3$ ) spectrum of compound  $\mathbf{15}^{\text{SCH}_3}$

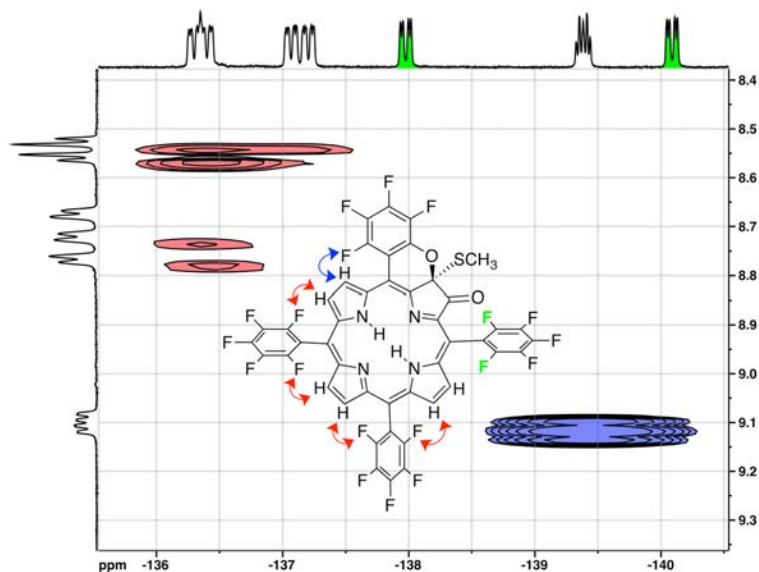


**Figure S40.**  $^1\text{H}$ - $^{19}\text{F}$  COSY NMR (400 MHz,  $\text{CDCl}_3$ ) spectrum of compound  $\mathbf{15}^{\text{SCH}_3}$

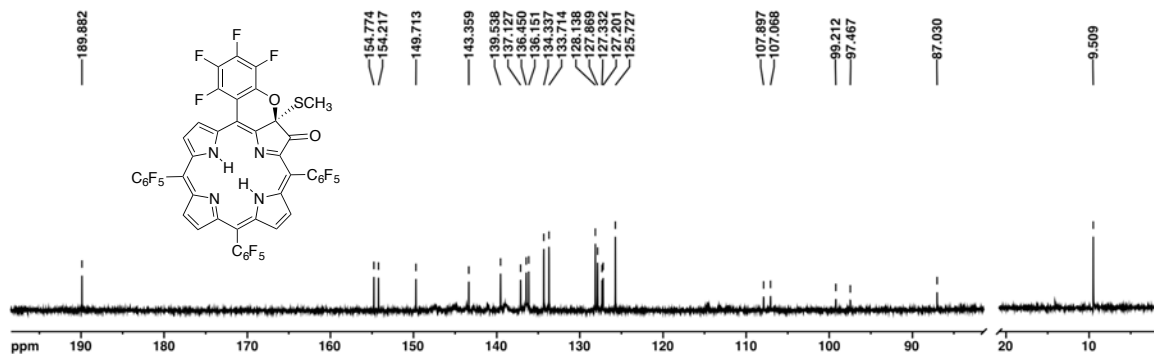


**Figure S41.**  $^{13}\text{C}$  NMR (100 MHz,  $\text{CDCl}_3$ ) spectrum of compound  $\mathbf{15}^{\text{SCH}_3}$

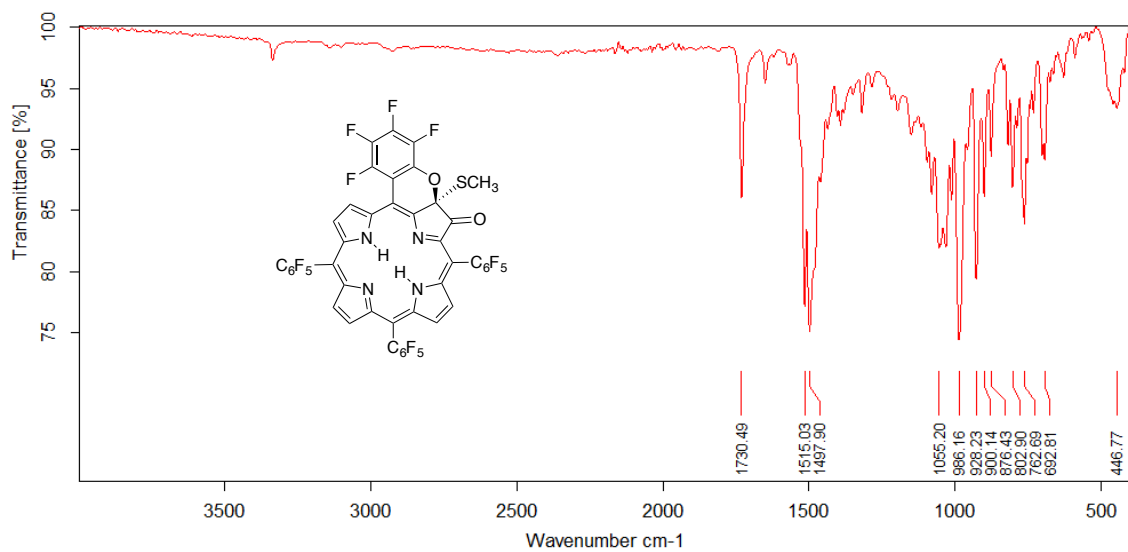


**Figure S42.** IR (neat, diamond ATR) spectrum of compound  $\mathbf{15}^{\text{SCH}_3}$

[10,15,20-Tris(pentafluorophenyl)-5-(tetrafluorochromene-annulated)-2-oxo-3-yl]dimer (**16**)

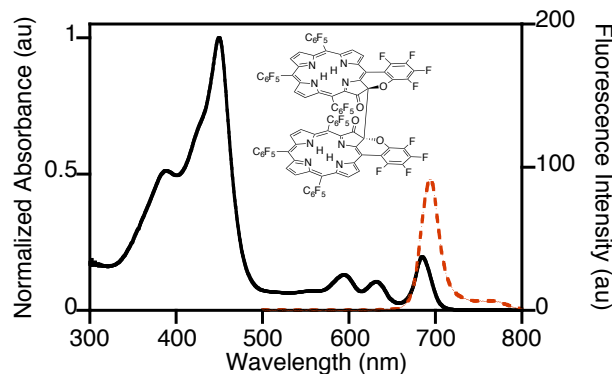


**Figure S43.** UV-Vis (black solid trace) and fluorescence (red dotted trace) spectra of dimer **16** ( $\text{CH}_2\text{Cl}_2$ );  $\lambda_{\text{excitation}} = \lambda_{\text{Soret}}$

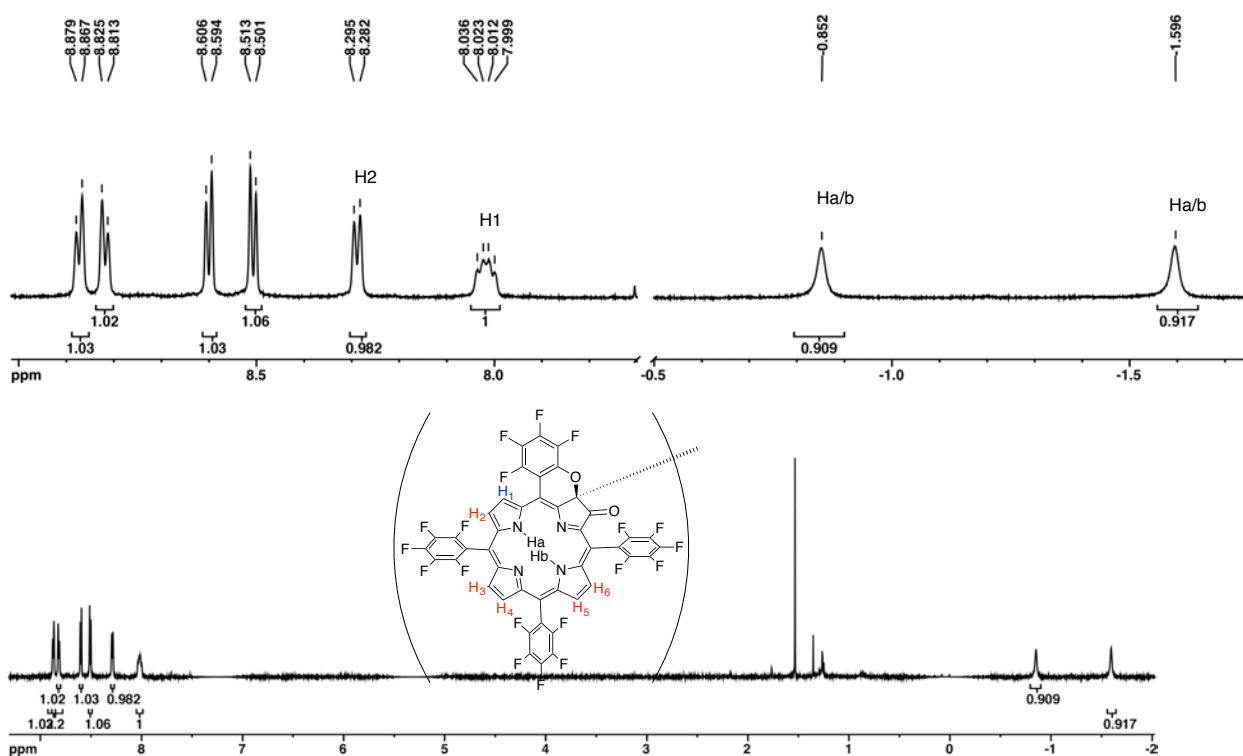


**Figure S44.**  $^1\text{H}$  NMR (400 MHz,  $\text{CDCl}_3$ ) spectrum of dimer **16**

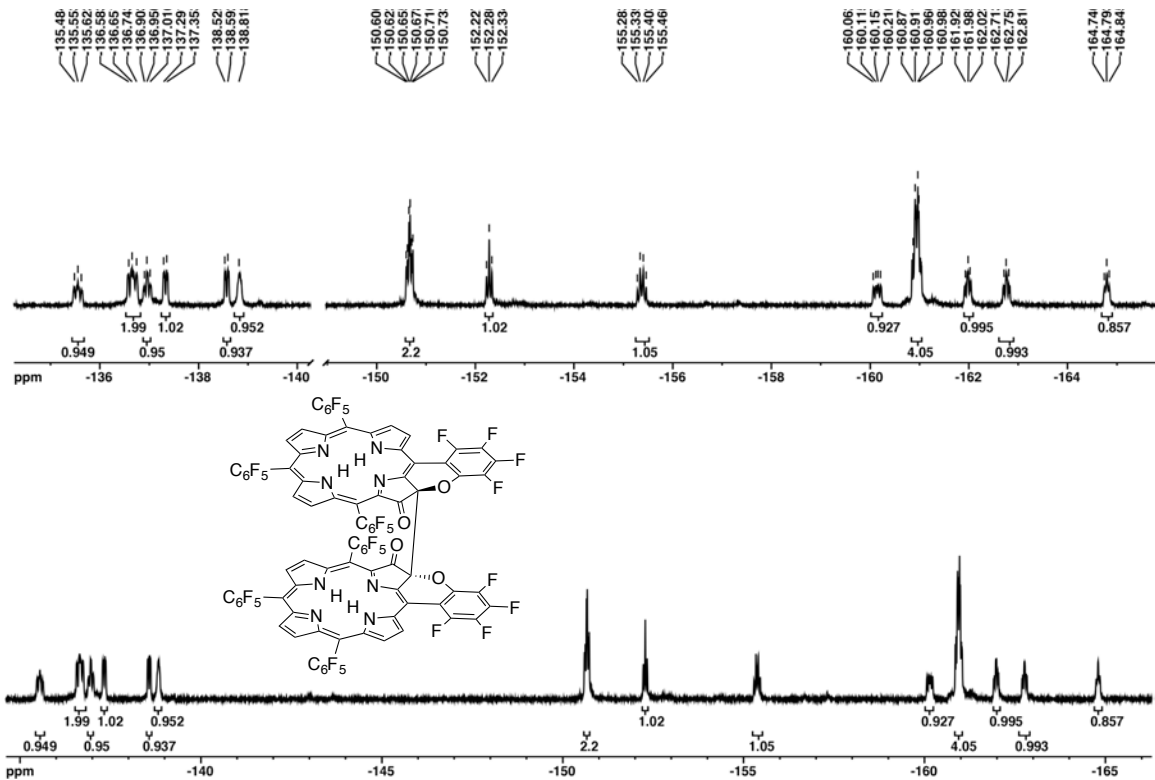


**Figure S45.**  $^{19}F$  NMR (376 MHz,  $CDCl_3$ ) spectrum of dimer **16**

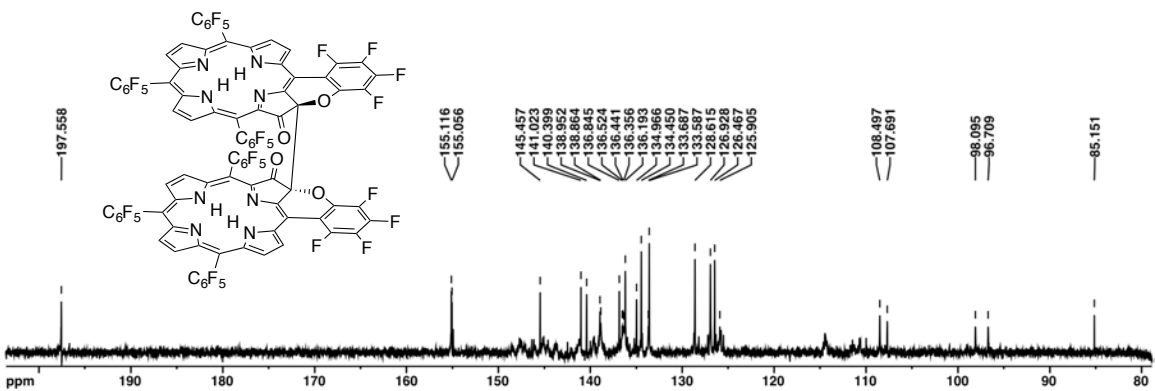


**Figure S46.**  $^{13}C$  NMR (100 MHz,  $CDCl_3$ ) spectrum of compound **16**

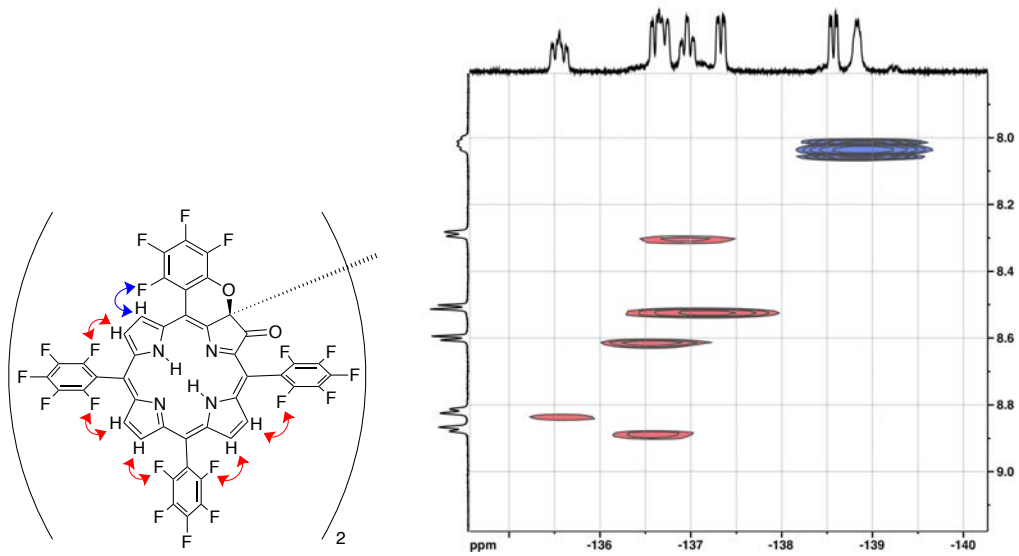


**Figure S47.**  $^1\text{H}$ - $^{19}\text{F}$  COSY NMR (400 MHz,  $\text{CDCl}_3$ ) spectrum of dimer **16**

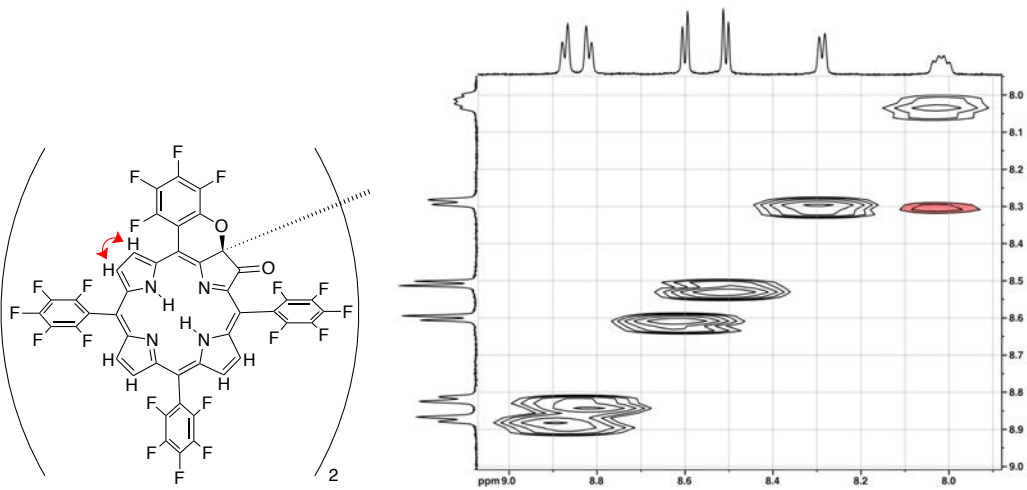


**Figure S48.**  $^1\text{H}$ - $^1\text{H}$  COSY NMR (400 MHz,  $\text{CDCl}_3$ ) spectrum of dimer **16**.

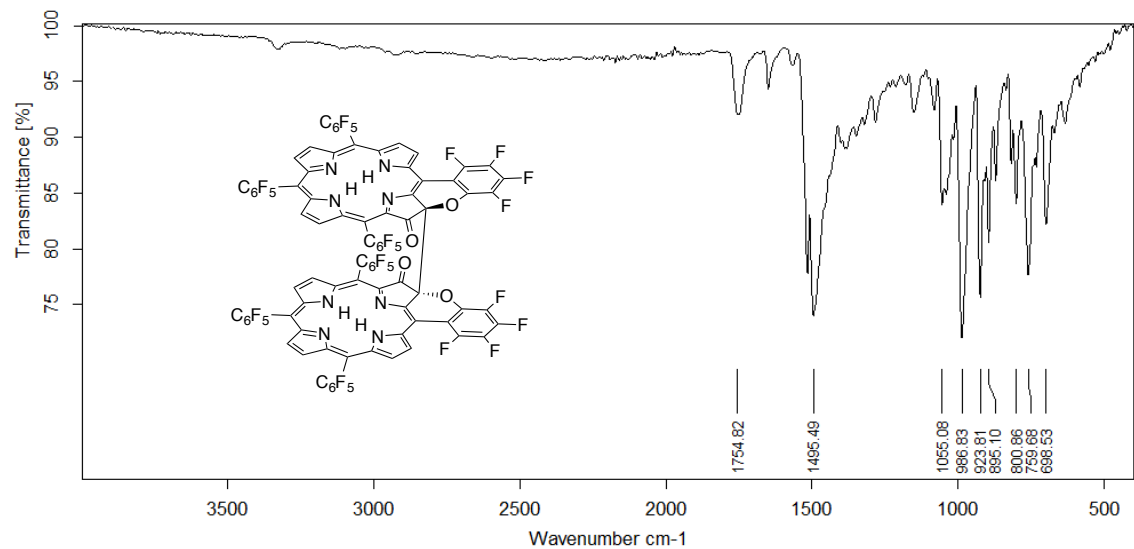


**Figure S49.** IR (neat, diamond ATR) spectrum of compound **16**

### Dimer (17)

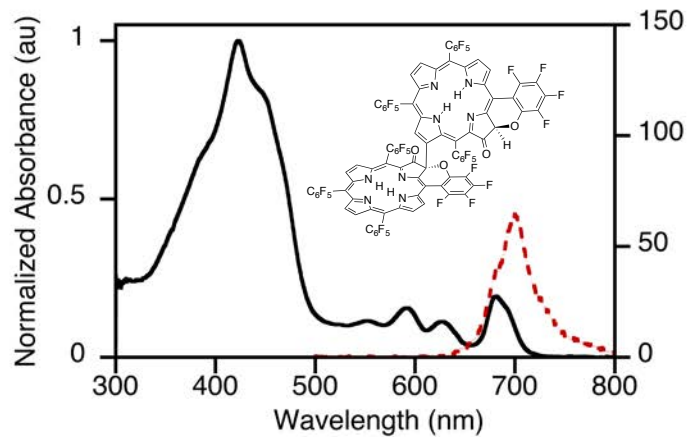


**Figure S50.** UV-Vis (black solid trace) and fluorescence (red dotted trace) spectra of dimer **17** ( $\text{CH}_2\text{Cl}_2$ );  $\lambda_{\text{excitation}} = \lambda_{\text{Soret}}$

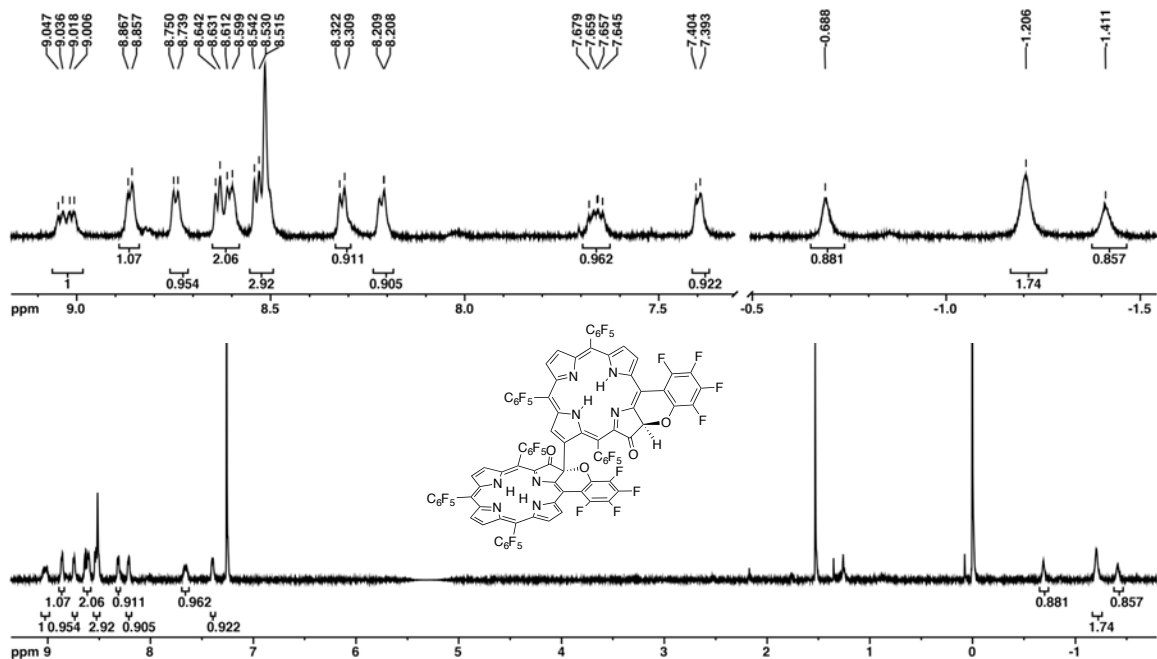


**Figure S51.** <sup>1</sup>H NMR (400 MHz, CDCl<sub>3</sub>) spectrum of dimer compound 17

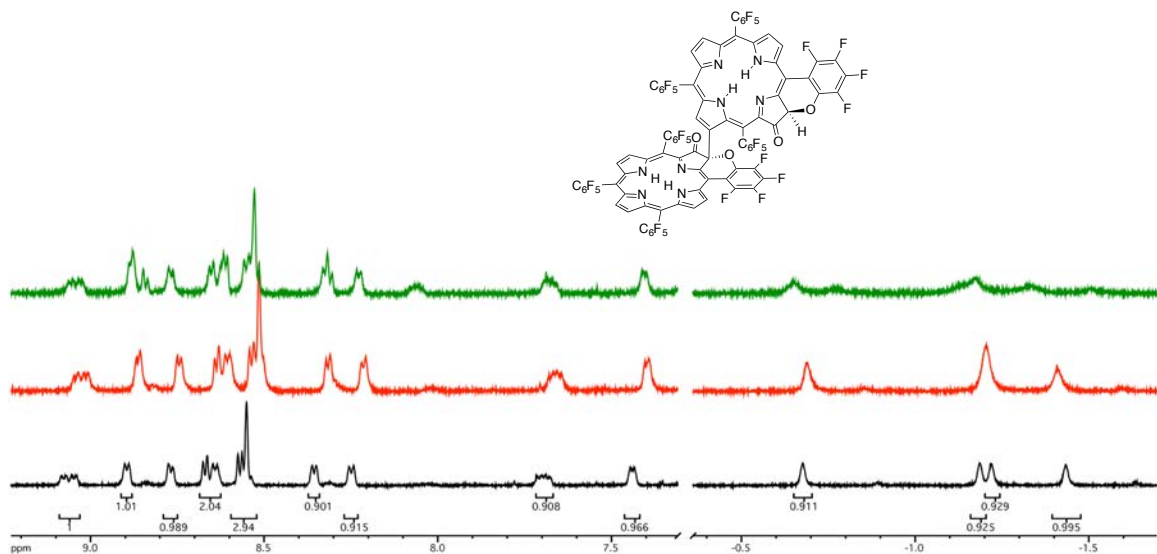


**Figure S52.** Temperature variable <sup>1</sup>H NMR (400 MHz, CDCl<sub>3</sub>) spectra of dimer compound 17: black trace 280K, red trace 300K and green trace 330K.

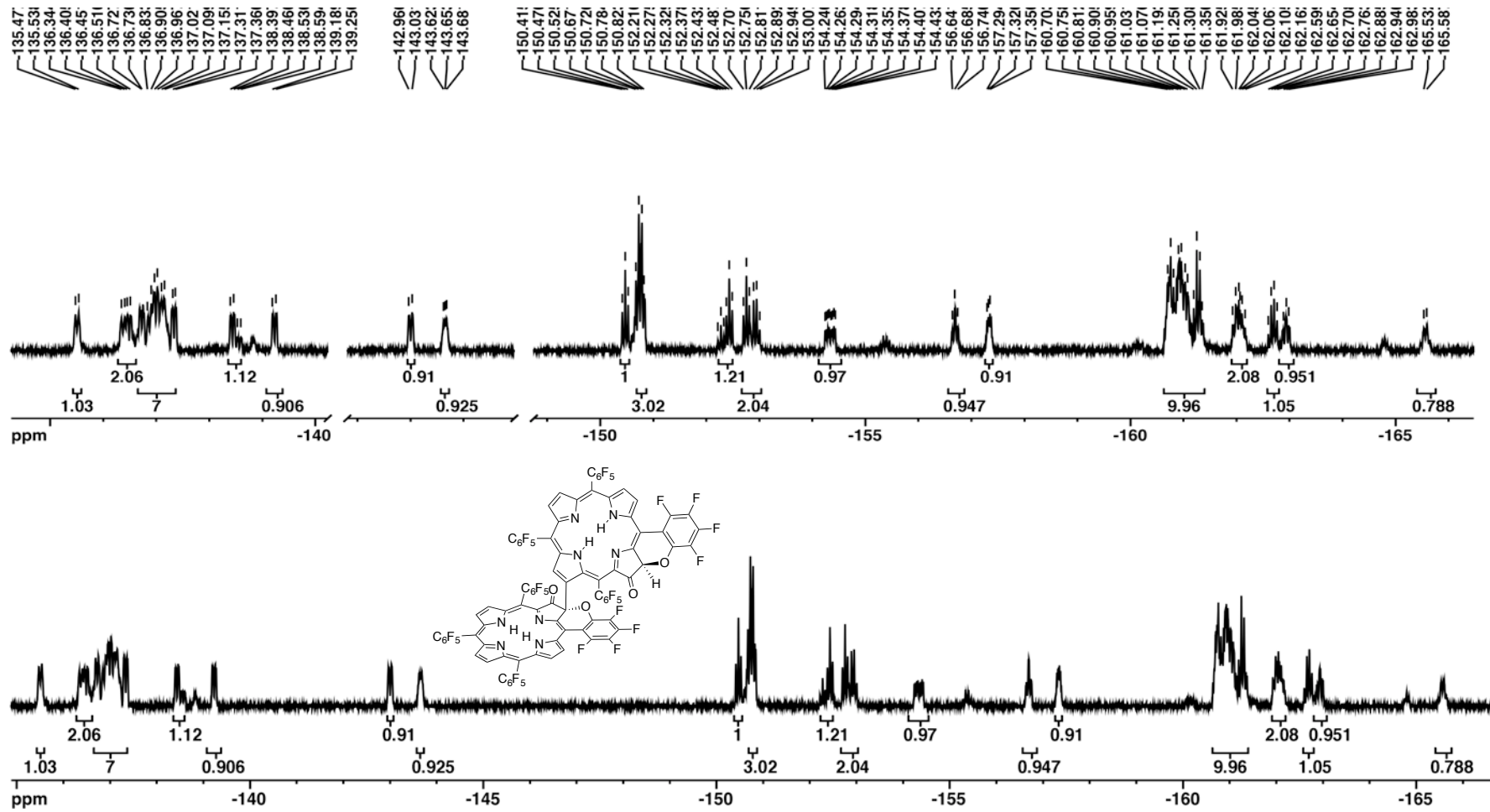


**Figure S53.**  $^{19}\text{F}$  NMR (376 MHz,  $\text{CDCl}_3$ ) spectrum of compound 17

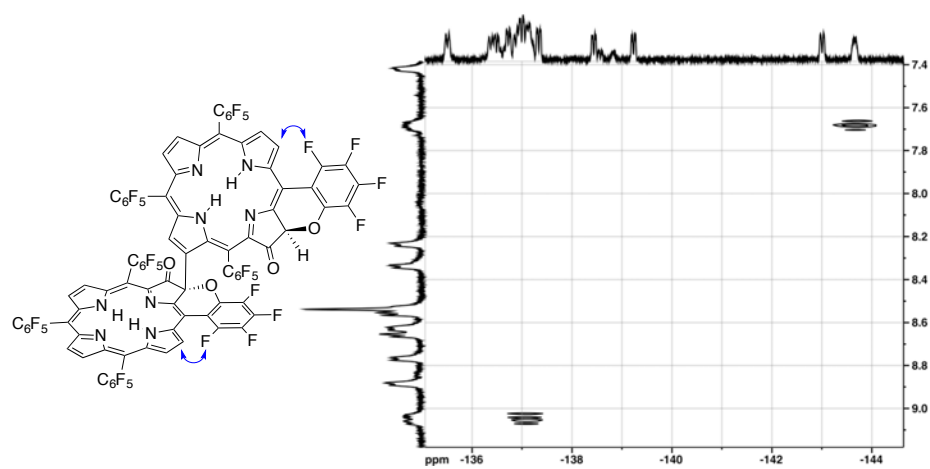


**Figure S54.**  $^1\text{H}$ - $^{19}\text{F}$  COSY NMR (400 MHz,  $\text{CDCl}_3$ ) spectrum of compound **17**

## NSD Analysis

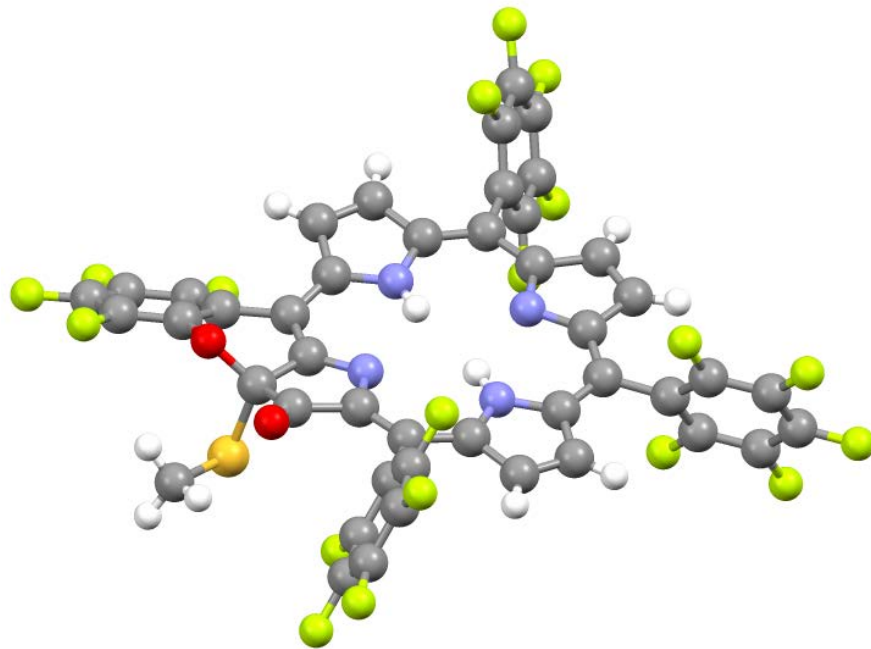


Table 1: NSD analysis of compound **15<sup>SCH<sub>3</sub></sup>-1** (In-plane displacement)

basis	Dip	dip	B2g	B1g	Eu(x)	Eu(y)	A1g	A2g
min.	0.2133	0.0265	-0.0284	-0.0846	0.0062	0.0322	0.1875	-0.036
ext.	0.2322	0.0197	-0.0283	-0.0859	0.0061	0.0316	0.1875	-0.0362
			0.0232	-0.0693	-0.0061	-0.0515	-0.0072	-0.0196
comp.	0.2614	0	0.0403	0.1404	0.0501	0.068	0.195	0.0432

Table 2: NSD analysis of compound **15<sup>SCH<sub>3</sub></sup>-1** (Out-of-plane displacement)

basis	Doop	doop	B2u	B1u	A2u	Eg(x)	Eg(y)	A1u
min.	0.665	0.0358	0.0802	-0.4851	-0.1143	-0.1084	-0.4019	0.1188
ext.	0.6898	0.0204	0.0803	-0.4851	-0.111	-0.1115	-0.3977	0.1188
			0.0055	0.0612	0.0761	-0.0821	0.1136	-0.0663
comp.	0.7022	0	0.0805	0.4908	0.1373	0.1389	0.4348	0.136

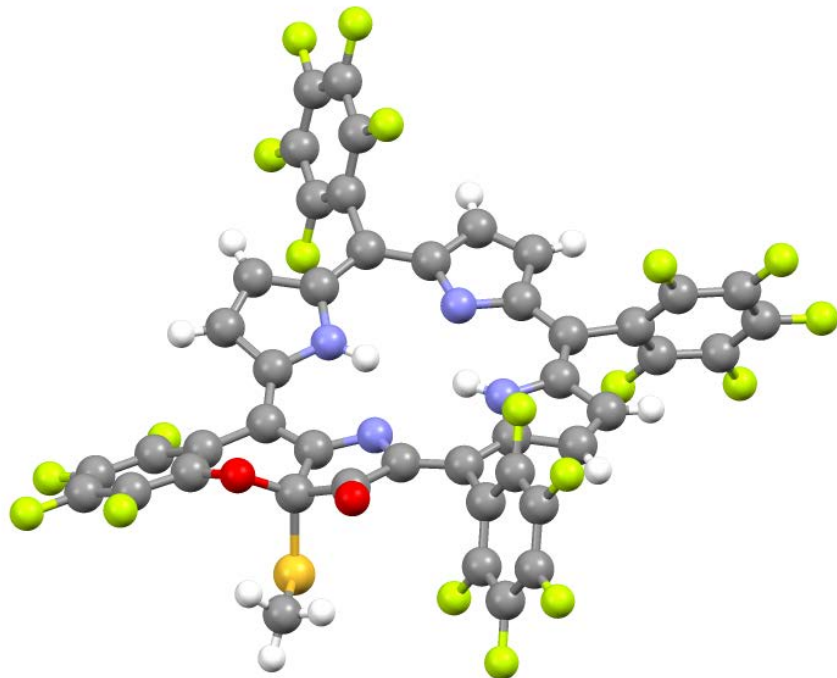


Table 3: NSD analysis of compound **15<sup>SCN</sup>-2** (In-plane displacement)

basis	Dip	dip	B2g	B1g	Eu(x)	Eu(y)	A1g	A2g
min.	0.1472	0.0339	-0.0193	-0.0637	0.0429	0.068	0.1011	-0.0234
ext.	0.1931	0.0239	-0.0189	-0.0653	0.0429	0.0674	0.1012	-0.0236
			0.0638	-0.0812	-0.005	-0.0522	0.0412	-0.0224
comp.	0.2401	0	0.0791	0.1296	0.0611	0.109	0.1323	0.0388

Table 4: NSD analysis of compound **15<sup>SCN</sup>-2** (Out-of-plane displacement)

basis	Doop	doop	B2u	B1u	A2u	Eg(x)	Eg(y)	A1u
min.	1.1671	0.0322	-0.0963	-1.0271	-0.2245	-0.3177	-0.3591	0.1327
ext.	1.1778	0.024	-0.0965	-1.0271	-0.2226	-0.3208	-0.3572	0.1327
			-0.0072	0.0902	0.0441	-0.0829	0.0499	-0.0743
comp.	1.1881	0	0.0978	1.0325	0.2288	0.3301	0.3892	0.152

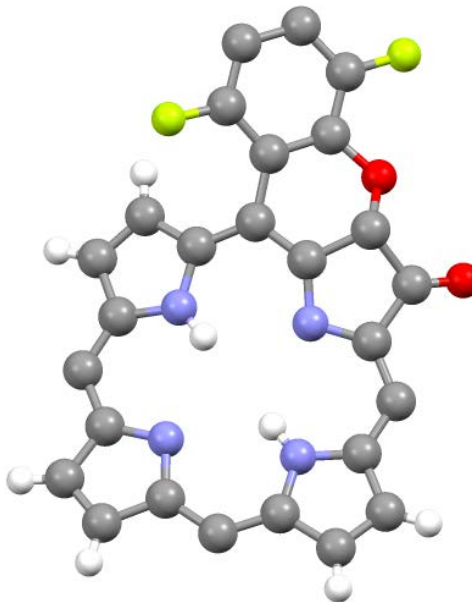


Table 5: NSD analysis of compound **16** (In-plane displacement)

basis	Dip	dip	B2g	B1g	Eu(x)	Eu(y)	A1g	A2g
min.	0.197	0.0314	0.0831	0.1421	0.041	-0.0702	0.065	-0.0298
ext.	0.2237	0.0233	0.083	0.1438	0.0409	-0.07	0.0651	-0.0295
			-0.0207	0.0858	-0.0041	0.0218	0.0433	0.0326
	0.2629	0	0.0858	0.1896	0.0506	0.0918	0.1128	0.0462
comp.	0.2897	0	0.0784	0.1285	0.1078	0.0776	0.1976	0.0676

Table 6: NSD analysis of compound **16** (Out-of-plane displacement)

basis	Doop	doop	B2u	B1u	A2u	Eg(x)	Eg(y)	A1u
min.	1.3156	0.0446	0.5304	1.0898	-0.0229	-0.4866	-0.0152	0.1557
ext.	1.3379	0.0267	0.5298	1.0898	-0.0221	-0.4796	-0.014	0.1557
			-0.0326	-0.1129	0.0183	0.1875	0.0327	-0.0932
	1.3495	0	0.5315	1.0973	0.0295	0.5471	0.0383	0.1815
comp.	0	0	0	0	0	0	0	0

## Crystallographic Details

### ***General Procedures.***

Data were collected using a Bruker AXS X8 Prospector CCD diffractometer with Cu-K $\alpha$  radiation with an I $\mu$ S microsource and a laterally graded multilayer (Goebel) mirror for monochromatization. Single crystals were mounted on Mitegen micromesh mounts using a trace of mineral oil and cooled in-situ to 100(2) K for data collection. Frames were collected, reflections were indexed and processed, and the files scaled and corrected for absorption using APEX2.<sup>2</sup> The space groups were assigned and the structures were solved by direct methods using XPREP within the SHELXTL suite of programs<sup>3</sup> and refined by full matrix least squares against  $F^2$  with all reflections using Shelxl2013 or 2014<sup>4</sup> and the graphical interface Shelxle.<sup>5</sup> H atoms attached to carbon and nitrogen atoms were positioned geometrically and constrained to ride on their parent atoms, with carbon hydrogen bond distances of 0.95 Å for alkene and aromatic C-H, 1.00, 0.99 and 0.98 Å for aliphatic C-H, CH<sub>2</sub> and CH<sub>3</sub>, and 0.88 Å for N-H moieties, respectively. Methyl H atoms were allowed to rotate but not to tip to best fit the experimental electron density. U<sub>iso</sub>(H) values were set to a multiple of U<sub>eq</sub>(C/N) with 1.5 for CH<sub>3</sub>, and 1.2 for C-H, CH<sub>2</sub> and N-H units, respectively. Details of disorder and other special considerations for each structure are given below and in the Crystallographic Information Files, CIFs. Complete crystallographic data, in CIF format, have been deposited with the Cambridge Crystallographic Data Centre. CCDC 1504764-1504766 contain the supplementary crystallographic data for this paper. These data can be obtained free of charge from The Cambridge Crystallographic Data Centre via [www.ccdc.cam.ac.uk/data\\_request/cif](http://www.ccdc.cam.ac.uk/data_request/cif).

---

(2) Apex2 v2014.1, Bruker AXS Inc.: Madison (WI), USA, 2009.

(3) (a) SHELXTL (Version 6.14) (2000-2003) Bruker Advanced X-ray Solutions, Bruker AXS Inc., Madison, Wisconsin: USA. (b) Sheldrick, G. M. *Acta Cryst. A* **2008**, *64*, 112-122.

(4) (a) Sheldrick, G. M. *Acta Cryst. C*, **2015**, *71*, 3-8. (b) Sheldrick, G. M. **2013**. University of Göttingen, Germany.

(5) Hübschle, C. B., Sheldrick, G. M. and Dittrich, B. *J. Appl. Cryst.*, **2011**, *44*, 1281-1284.

**Table 1. Experimental Details Crystallography**

Experiments were carried out at 100 K with Cu  $K\alpha$  radiation using a Bruker AXS X8 Prospector CCD diffractometer with an I- $\mu$ -S microsource X-ray tube and laterally graded multilayer (Goebel) mirror. Data collection used omega and phi scans. Absorption was corrected for by multi-scan methods, Apex2 v2014.11 (Bruker, 2014). H-atom parameters were constrained.

	<b>16</b> (YSU16mz010_0m)	<b>15</b> <sup>SCH<sub>3</sub></sup> (Prosp15mz169_0m)	<b>14-A/14-B</b> (NH- 125_Prosp15mz171_sq)
<b>Crystal data</b>			
Chemical formula	C <sub>88</sub> H <sub>16</sub> F <sub>38</sub> N <sub>8</sub> O <sub>4</sub> ·C <sub>6</sub> H <sub>14</sub>	C <sub>45</sub> H <sub>11</sub> F <sub>19</sub> N <sub>4</sub> O <sub>2</sub> S·0.651(CH <sub>2</sub> Cl <sub>2</sub> )·0.135(CH <sub>4</sub> S)	C <sub>43</sub> H <sub>9</sub> F <sub>19</sub> N <sub>4</sub> O <sub>3</sub>
<i>M</i> <sub>r</sub>	2057.26	1094.42	990.54
Crystal system, space group	Monoclinic, <i>I</i> 2/ <i>a</i>	Triclinic, <i>P</i> 1̄	Monoclinic, <i>I</i> 2/ <i>m</i>
<i>a</i> , <i>b</i> , <i>c</i> (Å)	13.7073 (6), 13.9417 (6), 41.647 (2)	15.894 (1), 16.7789 (10), 18.4175 (11)	7.5252 (7), 24.2334 (17), 15.7891 (16)
$\alpha$ , $\beta$ , $\gamma$ (°)	90, 90.1310 (16), 90	79.362 (2), 69.996 (2), 65.955 (2)	90, 90.167 (4), 90
<i>V</i> (Å <sup>3</sup> )	7958.9 (6)	4209.0 (5)	2879.3 (4)
<i>Z</i>	4	4	2
<i>F</i> (000)	4096	2171.4	980
<i>D</i> <sub>x</sub> (Mg m <sup>-3</sup> )	1.717	1.727	1.143
No. of refl. for cell measurement	9889	9523	4302
$\theta$ range (°) for cell measurement	3.3–66.6	2.9–66.9	3.3–66.1
$\mu$ (mm <sup>-1</sup> )	1.51	2.72	1.04
Crystal shape	Rod	Block	Plate
Colour	Black	Black	Black
Crystal size (mm)	0.25 × 0.10 × 0.08	0.25 × 0.20 × 0.14	0.37 × 0.20 × 0.04
<b>Data collection</b>			
<i>T</i> <sub>min</sub> , <i>T</i> <sub>max</sub>	0.603, 0.753	0.657, 0.753	0.564, 0.753
No. of measd, indep. and obs. [ <i>I</i> > 2σ( <i>I</i> )] reflections	19690, 6860, 6190	63719, 14572, 12701	7917, 2436, 1901
<i>R</i> <sub>int</sub>	0.042	0.027	0.068
$\theta$ values (°)	$\theta_{\text{max}} = 67.0$ , $\theta_{\text{min}} = 2.1$	$\theta_{\text{max}} = 66.8$ , $\theta_{\text{min}} = 2.6$	$\theta_{\text{max}} = 66.4$ , $\theta_{\text{min}} = 3.3$
(sin $\theta$ /λ) <sub>max</sub> (Å <sup>-1</sup> )	0.597	0.596	0.594
Range of <i>h</i> , <i>k</i> , <i>l</i>	<i>h</i> = -16→12, <i>k</i> = -15→16, <i>l</i> = -49→46	<i>h</i> = -18→18, <i>k</i> = -19→19, <i>l</i> = -21→21	<i>h</i> = -8→8, <i>k</i> = -28→26, <i>l</i> = -18→18

<b>Refinement</b>			
$R[F^2 > 2\sigma(F^2)]$ , $wR(F^2), S$	0.058, 0.160, 1.08	0.040, 0.102, 1.03	0.129, 0.396, 1.48
No. of reflections	6860	14572	2436
No. of parameters	650	1415	248
No. of restraints	0	186	526
	$w = 1/[\sigma^2(F_o^2) + (0.0705P)^2 + 35.7674P]$ where $P = (F_o^2 + 2F_c^2)/3$	$w = 1/[\sigma^2(F_o^2) + (0.0413P)^2 + 5.8592P]$ where $P = (F_o^2 + 2F_c^2)/3$	$w = 1/[\sigma^2(F_o^2) + (0.230P)^2]$ where $P = (F_o^2 + 2F_c^2)/3$
$\Delta\rho_{\max}, \Delta\rho_{\min}$ (e Å <sup>-3</sup> )	0.59, -0.32	0.60, -0.51	0.51, -0.36
CCDC #	1504765	1504766	1504764

Computer programs: Apex2 v2014.11 (Bruker, 2014), SAINT V8.34A (Bruker, 2014), SHELLXS97 (Sheldrick, 2008), SHELLXL2014/7 (Sheldrick, 2014), SHELLXLE Rev714 (Hübschle *et al.*, 2011).

*Crystallographic Details for 16*

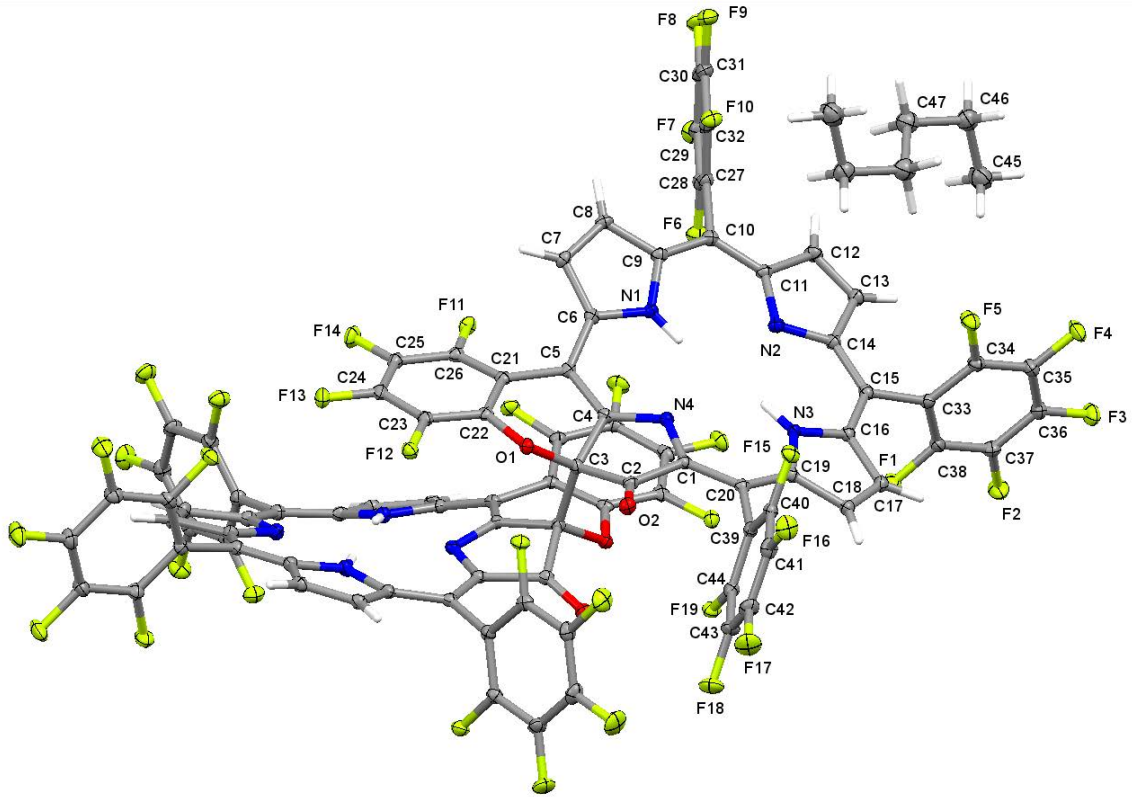


**Figure S55.** Thermal ellipsoid representation of YSU16mz010\_0m. Thermal parameters at the 50% probability level. Labels for symmetry created atoms omitted for clarity.

### *Crystallographic Details for $\mathbf{15}^{\text{SCH}_3}$*

For  $\mathbf{15}^{\text{SCH}_3}$ , pockets of electron density between porphorinoid molecules are filled with a mixture of disordered methylene chloride and methyl sulfide. One of the sites was modelled as occupied by methylene chloride in three different orientations, ignoring possibly present methyl sulfide. The other site was refined as being occupied by each one partially occupied methylene chloride and methyl sulfide molecule. All methylene chloride molecules were restrained to have similar geometries, and  $U_{ij}$  components of ADPs of disordered atoms were restrained to be similar if closer than 1.7 Å. Subject to these conditions, the occupancies of the three methylene chloride moieties refined to 0.482(3), 0.212(3) and 0.212(3), and the occupancies of the methyl sulfide and methylene chloride moieties to 0.270(5) and 0.511(3). Additional disorder or slightly different  $\text{CH}_2\text{Cl}_2$  to  $\text{HSMe}$  ratios are possible.

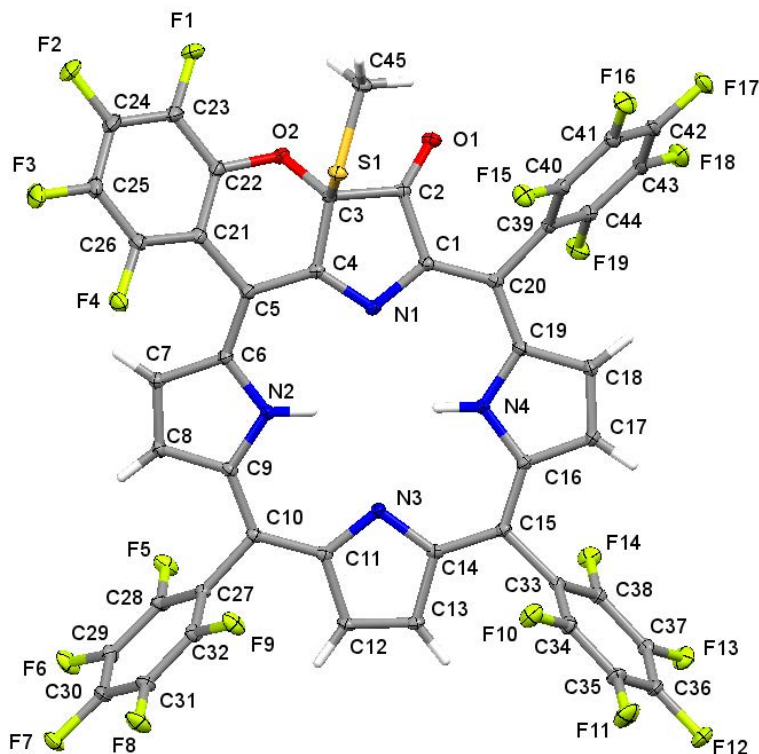


**Figure S56.** Thermal ellipsoid representation of the first of two independent molecules in  $\mathbf{15}^{\text{SCH}_3}$  (Prosp15mz169\_0m). Thermal parameters at the 50% probability level. H atom labels omitted for clarity.

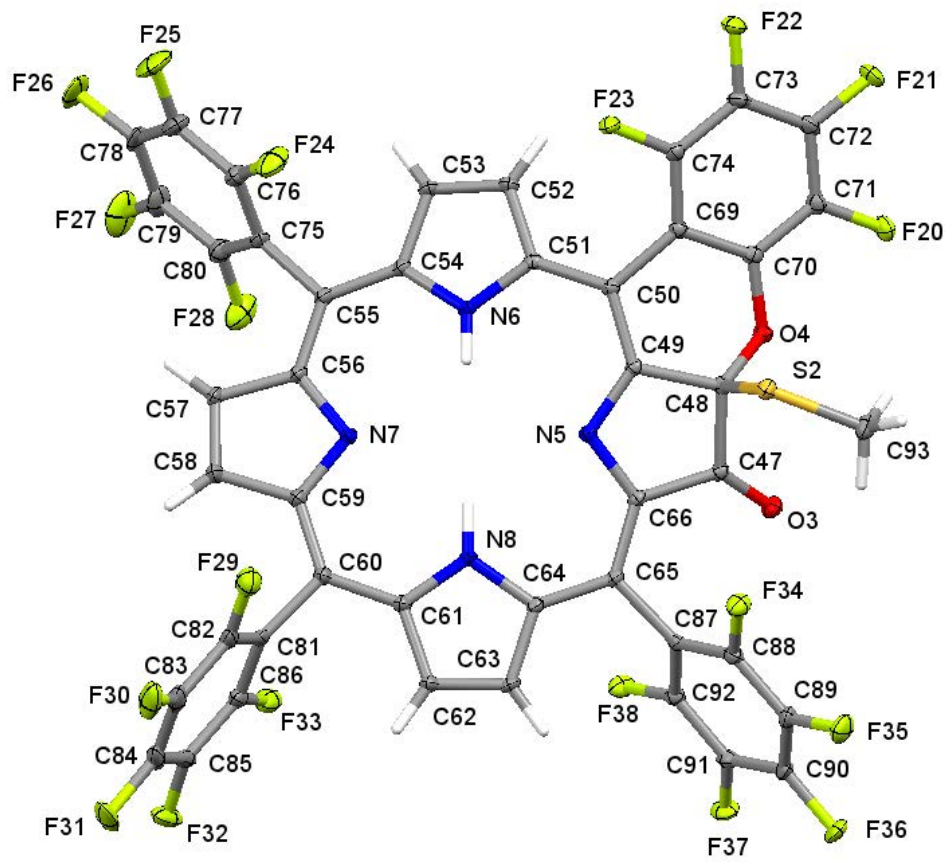


**Figure S57.** Thermal ellipsoid representation of the second of two independent molecules in  $^{15}\text{SCH}_3$  (Prosp15mz169\_0m). Thermal parameters at the 50% probability level. H atom labels omitted for clarity.

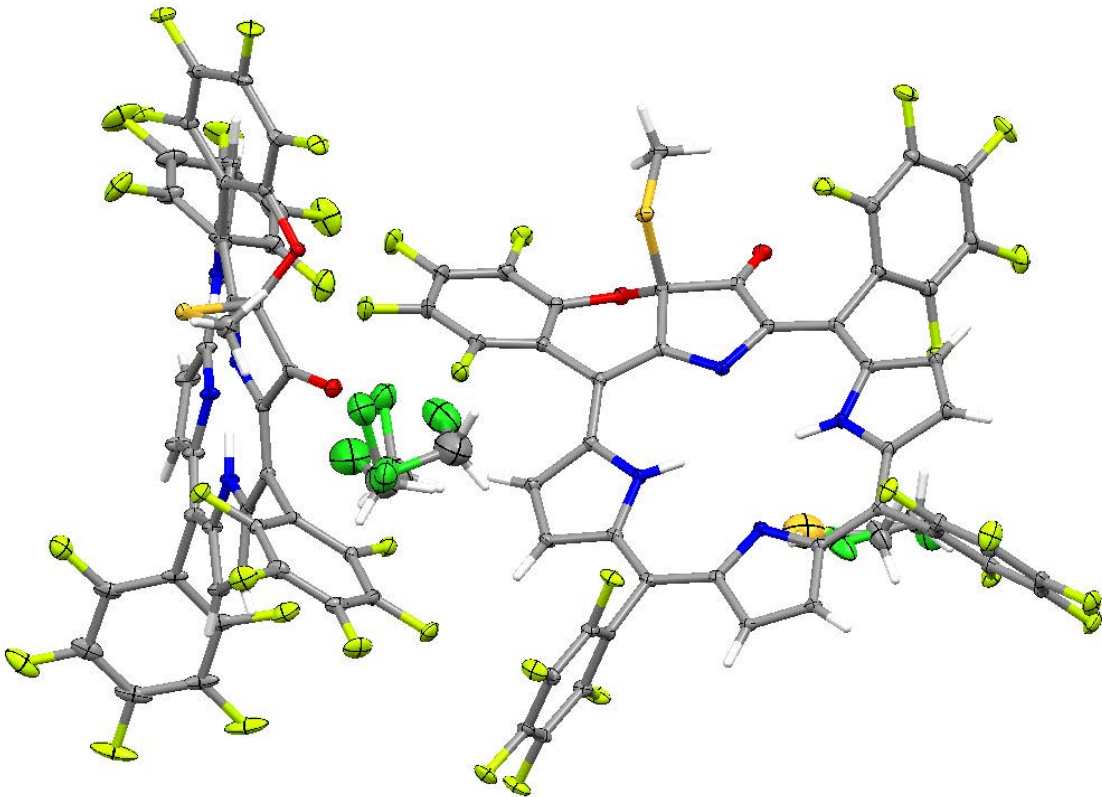


**Figure S58.** Thermal ellipsoid representation of **15<sup>SCH<sub>3</sub></sup>** (Prosp15mz169\_0m), showing both molecules and disordered solvate molecules. Thermal parameters at the 50% probability level. Labels are omitted for clarity.

### *Crystallographic Details for 14*

A single crystal structure of **14** further confirmed its ring-opened structure, but the structure is fraught by the presence of a 1:1 mixture of both possible isomers (**14-A/14-B**), complicated by extensive disorder. As observed in several other porpholactone crystal structures,<sup>6</sup> the lactone moiety of both isomers is distributed over two different positions, in two different orientations. The molecule is bisected by both a mirror plane and a twofold axis, rendering only one quarter of **14** crystallographically unique and inducing symmetry created fourfold disorder of the lactone moiety (over two positions in the porpholactone and mirror disordered in each position), and disorder of the tetrafluorohydroxy benzene ring with the three pentafluoro benzene rings over all meso positions. Thermal libration for the tetrafluorohydroxy and pentafluoro benzene rings is rather large. This, combined with the systematic symmetry imposed disorder, makes accurate assignment of the position of the hydroxyl group impossible and renders the determination of metric details challenging.

The structure has close to metric orthorhombic symmetry, emulating an I-centered orthorhombic lattice. It is twinned by that symmetry, twin law 1 0 0, 0 -1 0, 0 0 -1. Refinement as a 2-component twin yielded a twin ratio of 0.525(9) to 0.475(9).

The structure exhibits substantial disorder of both the lactone moiety and of the fluorinated benzene rings. The lactone moiety is 1:1 disordered with a pyrrole unit, and internally disordered with itself through a mirror plane, swapping the keto unit with the ring oxygen atom. The ring O atom the keto C atom and the C atoms of the pyrrole were constrained to have identical positions and ADPs (deviations of location and thermal parameter are not resolved within the accuracy of the measurement). The fluorinated benzene rings are substantially disordered via turns above or below the plane of the macrocycle. The disorder was modeled via a 0.75:0.25 disorder, following the disorder ratio of the lactone unit. The actual disorder of the fluorinated benzene rings is probably more complicated, but is not resolved within the accuracy of the measurement. The hydroxyl group was tentatively placed in the position closest to the keto oxygen atom as part of

---

6 (a) G. Khalil, M. Gouterman, S. Ching, C. Costin, L. Coyle, S. Gouin, E. Green, M. Sadilek, R. Wan, J. Yerryean, B. Zelelow, *J. Porphyrins Phthalocyanines* **2002**, *6*, 135-145. (b) C. Brückner, J. Ogikubo, J. R. McCarthy, J. Akhigbe, M. A. Hyland, P. Daddario, J. L. Worlinsky, M. Zeller, J. T. Engle, C. J. Ziegler, M. J. Ranaghan, M. N. Sandberg, R. R. Birge, *J. Org. Chem.* **2012**, *77*, 6480–6494.

the 25% occupied fluorinated benzene ring, but other locations are also possible.  $U_{ij}$  components of the ADPs of atoms of the fluorinated benzene rings were restrained to be similar if closer than 1.7 Å and to be close to isotropic (esd each 0.02 Å<sup>2</sup>). The hydroxyl oxygen atoms ADP was constrained to be identical to that of its fluorine counterpart in the major moiety fluorinated benzene ring. The position of the hydroxyl H atom was initially refined with a distance restrained of 2.76(2) Å to the keto O atom. In the final refinement cycles it was set to ride on the carrying oxygen atom.

Large parts of the unit cell volume are taken up by ill-defined solvate molecules (two times 19% of the unit cell volume, or 1095.7 Å<sup>3</sup>). No substantial electron density peaks were found in the solvent accessible voids (less than 2.15 electron per Å<sup>3</sup>) and the residual electron density peaks are not arranged in an interpretable pattern. The hkl file was instead corrected using reverse Fourier transform methods using the SQUEEZE routine (P. van der Sluis & A.L. Spek (1990). Acta Cryst. A46, 194-201) as implemented in the program Platon. The resultant files were used in the further refinement. (The FAB file with details of the Squeeze results is appended to the cif file). The Squeeze procedure corrected for 325.1 electrons within the solvent accessible voids.

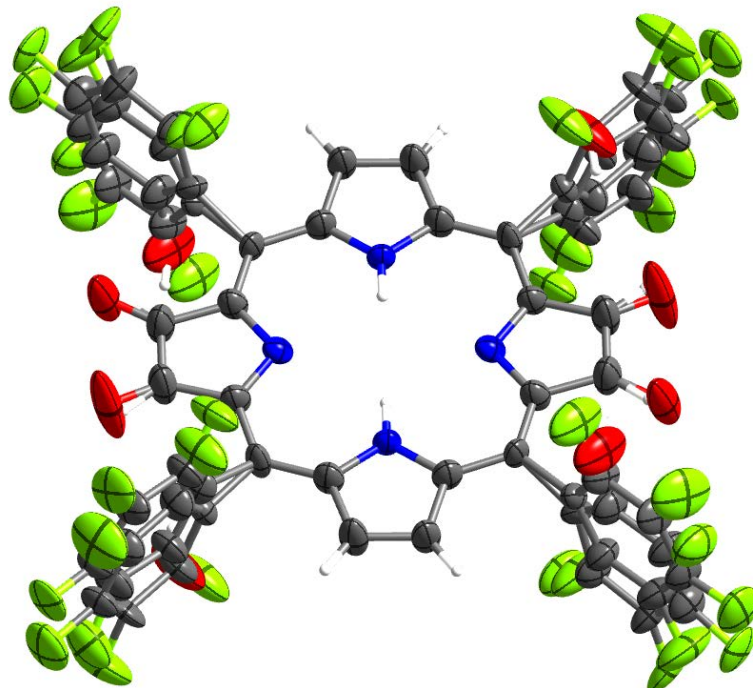


**Figure S59.** Thermal ellipsoid representation of **14-A/14-B** showing all disorder. Thermal parameters at the 50% probability level. All labels omitted for clarity.

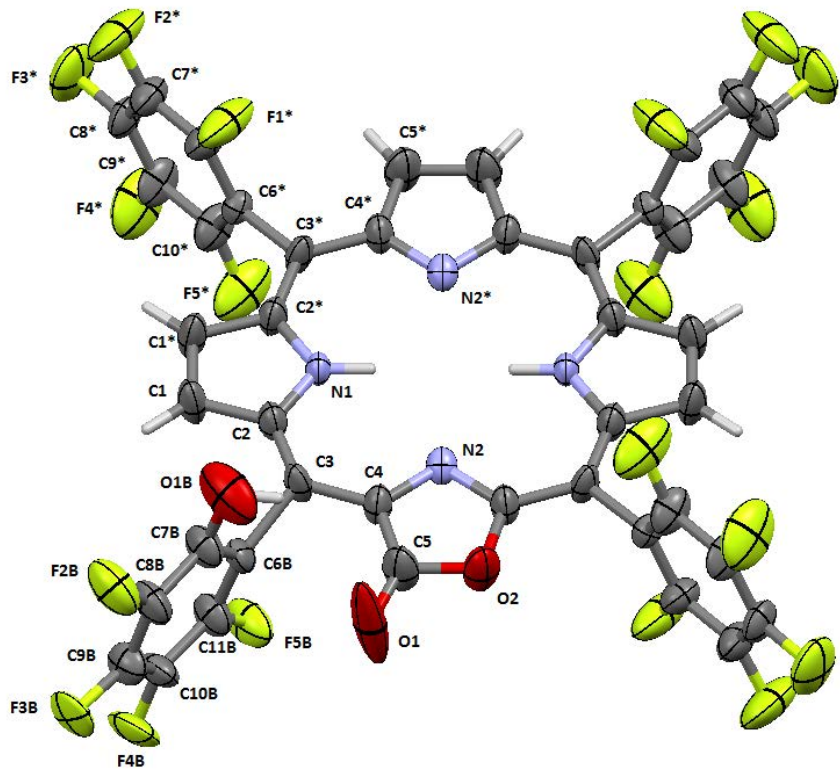


**Figure S60.** Thermal ellipsoid representation of **14** showing one molecule with all disorder omitted and half of all atoms labeled. Thermal parameters at the 50% probability level. Stared atoms \* are created by mirror symmetry, relating the upper and lower part of the molecule. Labels for all other atoms are omitted for clarity.